The Analytical One-Loop Contributions to Higgs Boson Mass in the Supersymmetric Standard Model with Vector-like Particles

Tianjun Li*[1,2], Wenyu Wang†[3], Xiao-Chuan Wang‡[1], and Zhao-Hua Xiong§[3]

[1]State Key Laboratory of Theoretical Physics, Institute of Theoretical Physics, Chinese Academy of Sciences, Beijing 100190, P. R. China

[2]School of Physical Electronics, University of Electronic Science and Technology of China, Chengdu 610054, P. R. China

[3]Institute of Theoretical Physics, Beijing University of Technology, Beijing 100124, P. R. China

June 26, 2015

Abstract

In the Minimal Supersymmetric Standard Model (MSSM) with additional vector-like particles (VLPs), we for the first time derive the particle mass spectra and the Feynman rules, as well as analytically calculate the one-loop contributions to the Higgs boson mass from the fermions and sfermions. After discussing and numerically analysing a cases without bilinear terms and a case with a (partial) decoupling limit, we find: (i) The corrections depend on the mass splittings between quarks and squarks and between vector-like fermions and their sfermions; (ii) There exists the (partial) decoupling limit, where the VLPs decouple from the electrwoeak (EW) energy scale, even when one of the VLPs is light around the EW scale. The reason is that the contributions to Higgs mass can be suppressed by the (or partial) decoupling effects, which can make the EW phenomenology very different from the MSSM; (iii) The SM-like Higgs boson with mass around 125 GeV gives strong constraints on the VLPs if the top squarks are around 1 TeV. Moreover, we present some numerical analyses to understand these unique features.

1 Introduction

With the observation of the Higgs boson [1, 2], the particle content of the electroweak Standard Model (SM) is confirmed by the experiments. In the future the main mission of Large Hedron Collider (LHC) is to measure the interactions involving Higgs precisely and search for the signatures of New Physics (NP). Among all the NP models, the Minimal Supersymmetric Standard Model (MSSM) is one of the

*tli@itp.ac.cn
†wywang@mail.itp.ac.cn
‡xcwang@itp.ac.cn
§xiongzh@ihep.ac.cn

most competitive candidates. It provides a natural solution to the gauge hierarchy problem in the SM and realizes the gauge coupling unification which strongly suggests Grand Unified Theories (GUTs). However, in GUTs there generically exists the doublet-triplet splitting problem and dimension-five proton decay problem. Fortunately, the flipped $SU(5) \times U(1)_X$ model [3, 4, 5] could elegantly solve these problems via missing partner mechanism [5]. In order to explain the little hierarchy problem between the traditional GUT scale and string scale, one of us (TL) with Jiang and Nanopoulos proposed the testable flipped $SU(5) \times U(1)_X$ model, dubbed as $\mathcal{F}$-$SU(5)$ [6], in which the TeV-scale vector-like particles (VLP) were introduced [7]. Such kind of models can be constructed from the free fermionic string constructions at the Kac-Moody level one [8, 9] and from the local F-theory model [10, 6]. These models are very interesting from the phenomenological point of view [6]: the VLPs could be observed at the Large Hadron Collider (LHC), proton decay is within the reach of the future Hyper-Kamiokande [11] and Deep Underground Science and Engineering Laboratory (DUSEL) [12] experiments [13, 14], the hybrid inflation could be realized naturally, the correct cosmic primordial density fluctuations could be got [15], and the lightest CP-even Higgs boson mass could be lifted [16, 17], etc. With no-scale boundary conditions at $SU(5) \times U(1)_X$ unification scale [18], one of us (TL) with Maxin, Nanopoulos and Walker have found an extraordinarily constrained "golden point" [19] and "golden strip" [20] that satisfied all the latest experimental constraints and has an imminently observable proton decay rate [13]. For a review of the recent progresses, please see Ref. [21].

With the TeV-scale VLPs, the $\mathcal{F}$-$SU(5)$ model is different from the MSSM at low energy. For example, there exist non-decoupling effects in the quark and lepton sectors, comparing with the two Higgs doublet (2HD) model. In Ref. [22], we studied the B physics processes in the quark sector of the $\mathcal{F}$-$SU(5)$ model, including the quark mass spectra, Feynman rules, new operators and Wilson coefficients. We found that rich VLP phenomenology needs to be studied further, in addition to the other effects of VLPs studied in Refs. [16, 23, 24, 25, 27, 28]. In this paper, we will extend our previous study and add vector-like particle multiplets to the MSSM, dubbing as the MSSMV. In order to show the physics of VLPs more clearly, we concentrate on the changes compared with the MSSM. It is well-known that only Yukawa interactions generate the masses for quarks and leptons in both the SM and MSSM. However, if there are VLPs in models, the fermions could obtain their vector-like masses via the additional bilinear mass terms. The interaction vertices will be changed as well, so the Feynman rules and mass spectra are different from the MSSM. We will discuss their implications on loop corrections to the Higgs mass, (partial) decoupling suppression of fermion and sfermion sector, and whether there exist the non-decoupling effects at the EW scale, etc.

This paper is organized as follows. A brief description of our model, the mass matrices of all particles, and all Feynman rules of fermions and sfermions are presented in Section 2. Section 3 includes a complete analytical formula of the leading order one-loop correction to the Higg mass in the MSSMV in the on-shell renormalization scheme, and some numerical analyses. Section 4 is our summary.

2 The MSSMV

2.1 The Superpotential and Soft Terms

In this subsection, we present a brief description of the MSSMV. In addition to all the particles in the MSSM, we introduce two sets of vector-like quarks and leptons (one set with X ahead, the other set with

Y ahead) and they have opposite SM quantum numbers, as given in Table 1 [1].

SF	Spin 0	Spin $\frac{1}{2}$	Generations	$(U(1) \otimes \mathrm{SU}(2) \otimes \mathrm{SU}(3))$
$\hat{X}q$	$\tilde{X}q$	Xq	1	$(\frac{1}{6}, \mathbf{2}, \mathbf{3})$
$\hat{X}l$	$\tilde{X}l$	Xl	1	$(-\frac{1}{2}, \mathbf{2}, \mathbf{1})$
$\hat{Y}q$	$\tilde{Y}q$	Yq	1	$(-\frac{1}{6}, \mathbf{2}, \overline{\mathbf{3}})$
$\hat{Y}l$	$\tilde{Y}l$	Yl	1	$(\frac{1}{2}, \mathbf{2}, \mathbf{1})$
$\hat{X}d$	$X\tilde{d}_R^*$	Xd_R^*	1	$(\frac{1}{3}, \mathbf{1}, \overline{\mathbf{3}})$
$\hat{X}u$	$X\tilde{u}_R^*$	Xu_R^*	1	$(-\frac{2}{3}, \mathbf{1}, \overline{\mathbf{3}})$
$\hat{Y}d$	$Y\tilde{d}_R^*$	Yd_R^*	1	$(-\frac{1}{3}, \mathbf{1}, \mathbf{3})$
$\hat{Y}u$	$Y\tilde{u}_R^*$	Yu_R^*	1	$(\frac{2}{3}, \mathbf{1}, \mathbf{3})$
$\hat{X}e$	$X\tilde{e}_R^*$	Xe_R^*	1	$(1, \mathbf{1}, \mathbf{1})$
$\hat{Y}e$	$Y\tilde{e}_R^*$	Ye_R^*	1	$(-1, \mathbf{1}, \mathbf{1})$

Table 1: The extra VLPs and their Quantum Numbers.

It is clear that the X-type particles have the same quantum numbers as the SM fermions, so we could combine these X-type particles with ordinary three generation particles to shorten the superpotential, which is given by

$$\begin{aligned} W &= \mu \hat{H}_u \hat{H}_d - Y_d \hat{d} \hat{q} \hat{H}_d - Y_e \hat{e} \hat{l} \hat{H}_d + Y_u \hat{u} \hat{q} \hat{H}_u \\ &+ Y_{y_d} \hat{Y}d \hat{Y}q \hat{H}_u + Y_{y_e} \hat{Y}e \hat{Y}l \hat{H}_u - Y_{y_u} \hat{Y}u \hat{Y}q \hat{H}_d \\ &+ M_{y_q} \hat{q} \hat{Y}q + M_{y_u} \hat{u} \hat{Y}u + M_{y_d} \hat{d} \hat{Y}d + M_{y_l} \hat{l} \hat{Y}l + M_{y_e} \hat{e} \hat{Y}e, \end{aligned} \tag{1}$$

where $\hat{H}_d = (H_d^0, H_d^-)$ and $\hat{H}_u = (H_u^+, H_u^0)$ are the $SU(2)$ Higgs doublets with hypercharges $-1/2$ and $1/2$ and have vacuum expectation values (VEVs) $(v_d, 0)$ and $(0, v_u)$ $(\tan\beta = v_u/v_d)$, respectively. We emphasize that in this superpotential Y_d, Y_u, and Y_e are 4×4 matrices, and M_{y_q}, M_{y_u}, M_{y_d}, M_{y_l} and M_{y_e} are 4×1 matrices. So in Eq. (1) the first line are the superpotential which is the same as the MSSM in format. The second line are terms involving Y-type VLPs and the third line are the bilinear terms with mass dimensional matrix M_{y_q}, M_{y_u}, M_{y_d}, M_{y_l}, and M_{y_e} as input parameters. Compared with the MSSM, they are new terms in the MSSMV. We will concentrate on the implications of these terms in the following Section. The package SARAH4 [29] is used.

The next ingredient is the supersymmetry breaking soft terms. The gaugino masses are

$$-\mathcal{L}_{SB,\lambda} = \frac{1}{2}\Big(M_1 \lambda_{\tilde{B}}^2 + M_2 \lambda_{\tilde{W}}^2 + M_3 \lambda_{\tilde{g}} \lambda_{\tilde{g}} + \text{h.c.}\Big), \tag{2}$$

the scalar masses are

$$\begin{aligned} -\mathcal{L}_{SB,\phi} &= m_{H_d}^2 |H_d^0|^2 + m_{H_d}^2 |H_d^-|^2 + m_{H_u}^2 |H_u^0|^2 + m_{H_u}^2 |H_u^+|^2 \\ &+ m_q^2 |\tilde{u}_L|^2 + m_u^2 |\tilde{u}_R|^2 + m_q^2 |\tilde{d}_L|^2 + m_d^2 |\tilde{d}_R|^2 + m_l^2 |\tilde{e}_L|^2 + m_e^2 |\tilde{e}_R|^2 \\ &+ m_{Yq}^2 |\tilde{Y}u_L|^2 + m_{Yu}^2 |\tilde{Y}u_R|^2 + m_{Yq}^2 |\tilde{Y}d_L|^2 + m_{Yd}^2 |\tilde{Y}d_R|^2 \\ &+ m_{Yl}^2 |\tilde{Y}e_L|^2 + m_{Ye}^2 |\tilde{Y}e_R|^2 \ , \end{aligned} \tag{3}$$

[1] Although we can introduce more vector-like particles to the Lagrangian, because they will have similar mass spectra and Feynman rules, we only need to add more subscripts to the rotation matrix. Thus, we think it is enough to introduce only one generation at current stage.

and the trilinear soft terms are

$$
\begin{aligned}
-\mathcal{L}_{SB,W} &= -H_d^0 H_u^0 B_\mu \mu + H_d^- H_u^+ B_\mu \mu \\
&+ H_d^0 \tilde{d}_R^* \tilde{d}_L A_d - H_d^- \tilde{d}_R^* \tilde{u}_L A_d + H_d^0 \tilde{e}_R^* \tilde{e}_L A_e - H_d^- \tilde{e}_R^* \tilde{\nu}_L A_e + H_u^0 \tilde{u}_R^* \tilde{u}_L A_u - H_u^+ \tilde{u}_R^* \tilde{d}_L A_u \\
&+ H_u^0 \tilde{Y d}_R^* \tilde{Y d}_L A_{y_d} - H_u^+ \tilde{Y d}_R^* \tilde{Y u}_L A_{y_d} + H_u^0 \tilde{Y e}_L \tilde{Y e}_R^* A_{y_e} - H_u^+ \tilde{Y \nu}_L \tilde{Y e}_R^* A_{y_e} \\
&+ H_d^0 \tilde{Y u}_R^* \tilde{Y u}_L A_{y_u} - H_d^- \tilde{Y u}_R^* \tilde{Y d}_L A_{y_u} + \tilde{X u}_L \tilde{Y u}_L B_{M y_q} M_{y_q} + \tilde{X u}_R^* \tilde{Y u}_R^* B_{M y_u} M_{y_u} \\
&- \tilde{X d}_L \tilde{Y d}_L B_{M y_q} M_{y_q} + \tilde{X d}_R^* \tilde{Y d}_R^* B_{M y_d} M_{y_d} - \tilde{Y e}_L \tilde{X e}_L B_{M y_l} + \tilde{Y e}_R^* \tilde{X e}_R^* B_{M y_e} M_{y_e} + \text{h.c.}. \qquad (4)
\end{aligned}
$$

The Lagrangian characterizing the fermion, sfermion and gaugino interactions is

$$
\begin{aligned}
-\mathcal{L}_{F,SF,G} = &- \left[\frac{g_2}{\sqrt{2}} \left(\bar{u}_L^i,\ \bar{d}_L^i \right) \lambda_{\tilde{W},a} \sigma_{ij}^a \begin{pmatrix} \tilde{u}_L^j \\ \tilde{d}_L^j \end{pmatrix} + \frac{2}{3} \frac{g_1}{\sqrt{2}} \bar{u}_R^i \lambda_{\tilde{B}} \delta_{ij} \tilde{u}_R^j - \frac{1}{3} g_1 \sqrt{2} \bar{d}_R^i \lambda_{\tilde{B}} \delta_{ij} \tilde{d}_R^j + \text{h.c.} \right] \\
&- \left[\frac{g_2}{\sqrt{2}} \left(\overline{Yd}_L,\ \overline{Yu}_L \right) \lambda_{\tilde{W},a} \sigma^a \begin{pmatrix} \tilde{Yd}_L \\ \tilde{Yu}_L \end{pmatrix} + \frac{1}{3} \frac{g_1}{\sqrt{2}} \overline{Yd}_R \lambda_{\tilde{B}} \tilde{Yd}_R^j - \frac{2}{3} g_1 \sqrt{2} \overline{Yu}_R \lambda_{\tilde{B}} \tilde{Yu}_R^j + \text{h.c.} \right], \qquad (5)
\end{aligned}
$$

in which the terms in the first line are same as the MSSM in form, and the second line has the terms introduced by the Y-type VLPs which are the new terms in the MSSMV.

Generally the constants μ, B_μ, Yukawa matrices, squark and gaugino masses, bilinear matrices and the trilinear soft terms may be complex. One can eliminate the non-physical degrees of freedom by redefining the global phases of the fields. For example, the Higgs multiplets could be redefined so that the constant B_μ becomes a real number. Then the minimization equations for the VEVs of the Higgs fields will only involve real parameters. After the proper redefinition of the parameters, the rotation matrices of quarks and leptons still remain in the Lagrangian, leaving only a Kobayashi-Maskawa like matrix and tree-level Flavor-Changing Neutral Currents (FCNC) interactions.

2.2 The Particle Spectra

To obtain the physical spectra of particles present in the MSSMV one should carry out the standard procedure of gauge symmetry breaking via the VEVs of the neutral Higgs fields and calculate the eigenstates of the mass matrices for all fields. The Higgs and gaugino sectors in the MSSMV at tree level is the same as the MSSM, whereas only the fermion and sfermion sectors are different. The mass spectra of fermions and sfermions are given as follows

- Fermion Mass Matrices

With the participation of VLPs, the 3×3 quark/lepton mass matrices become the 5×5 mass matrices

$$
m_d = \begin{pmatrix} \frac{1}{\sqrt{2}} v_d Y_d^T & -M_{y_q,o_1}^T \\ M_{y_d,p_1} & \frac{1}{\sqrt{2}} v_u Y_{y_d} \end{pmatrix}, \quad m_u = \begin{pmatrix} \frac{1}{\sqrt{2}} v_u Y_u^T & M_{y_q,o_1}^T \\ M_{y_u,p_1} & \frac{1}{\sqrt{2}} v_d Y_{y_u} \end{pmatrix}, \quad m_e = \begin{pmatrix} \frac{1}{\sqrt{2}} v_d Y_e^T & -M_{y_l,o_1}^T \\ M_{y_e,p_1} & \frac{1}{\sqrt{2}} v_u Y_{y_e} \end{pmatrix}. \qquad (6)
$$

The X-type fermions can be considered as the fourth generation, and the mixings between the X-type and ordinary fermions give the upper left 4×4 elements of the matrices. The Y-type fermions give a different form in comparison with the fifth generation. Especially, the bilinear mass parameters M_{yq} connect the mass matrices of up-type and down-type quarks, so their diagonaliztions are not as simple as the MSSM. We use the following convention for the diagonalization

$$
U_L^{f\dagger} m_f U_R^f = m_f^{diag.}, \qquad (7)
$$

in which $U^{f}_{L,R}$ represent the rotation matrices and the superscript f represents $d,\ u,$ and e.

- Sfermion Mass Matrices

The squark and slepton mass matrices are extended from 6×6 to 10×10. The mass matrices for up-type squarks are given by

$$m^2_{\tilde{u}} = \begin{pmatrix} m_{\tilde{u}_L\tilde{u}^*_L} & m_{\tilde{u}_R\tilde{u}^*_L} & B^*_{My_q,o_1}M_{y_q,o_1} & m_{\tilde{Y}u^*_R\tilde{u}^*_L} \\ m_{\tilde{u}_L\tilde{u}^*_R} & m_{\tilde{u}_R\tilde{u}^*_R} & m_{\tilde{Y}u^*_L\tilde{u}^*_R} & B_{My_u,o_2}M_{y_u,o_2} \\ B_{My_q,p_1}M_{y_q,p_1} & m_{\tilde{u}_R\tilde{Y}u_L} & m_{\tilde{Y}u^*_L\tilde{Y}u_L} & m_{\tilde{Y}u^*_R\tilde{Y}u_L} \\ m_{\tilde{u}_L\tilde{Y}u_R} & B^*_{My_u,p_2}M_{y_u,p_2} & m_{\tilde{Y}u^*_L\tilde{Y}u_R} & m_{\tilde{Y}u^*_R\tilde{Y}u_R} \end{pmatrix} \tag{8}$$

with

$$\begin{aligned}
m_{\tilde{u}_L\tilde{u}^*_L} &= -\frac{1}{24}\Big(-3g_2^2+g_1^2\Big)\Big(-v_u^2+v_d^2\Big)+\frac{1}{2}\Big(2\Big(M_{y_q,o_1}M_{y_q,p_1}+m_q^2\Big)+v_u^2Y_u^\dagger Y_u\Big),\\
m_{\tilde{u}_R\tilde{u}^*_L} &= \frac{1}{\sqrt{2}}\Big(-v_dY_u^\dagger\mu+v_uA_u^\dagger\Big),\\
m_{\tilde{Y}u^*_R\tilde{u}^*_L} &= \frac{1}{\sqrt{2}}\Big(v_dY_{y_u}M_{y_q,o_1}+v_uY^*_{u,o_1}M_{y_u}\Big),\\
m_{\tilde{u}_L\tilde{u}^*_R} &= \frac{1}{\sqrt{2}}\Big(-v_dY_u\mu^*+v_uA_u\Big),\\
m_{\tilde{u}_R\tilde{u}^*_R} &= \frac{1}{2}\Big(2\Big(M_{y_u,o_2}M_{y_u,p_2}+m_u^2\Big)+v_u^2Y_uY_u^\dagger\Big)+\frac{1}{6}g_1^2\Big(-v_u^2+v_d^2\Big),\\
m_{\tilde{Y}u^*_L\tilde{u}^*_R} &= \frac{1}{\sqrt{2}}\Big(v_dY_{y_u}M_{y_u,o_2}+v_uM_{y_q}Y_{u,o_2}\Big),\\
m_{\tilde{u}_R\tilde{Y}u_L} &= \frac{1}{\sqrt{2}}\Big(v_dY_{y_u}M_{y_u,p_2}+v_uM_{y_q}Y^*_{u,p_2}\Big),\\
m_{\tilde{Y}u^*_L\tilde{Y}u_L} &= \frac{1}{24}\Big(-3g_2^2+g_1^2\Big)\Big(-v_u^2+v_d^2\Big)+\frac{1}{2}\Big(2\Big(m^2_{Yq}+M^2_{y_q}\Big)+v_d^2Y^2_{y_u}\Big),\\
m_{\tilde{Y}u^*_R\tilde{Y}u_L} &= \frac{1}{\sqrt{2}}\Big(v_dA_{y_u}-v_uY_{y_u}\mu^*\Big),\\
m_{\tilde{u}_L\tilde{Y}u_R} &= \frac{1}{\sqrt{2}}\Big(v_dY_{y_u}M_{y_q,p_1}+v_uY_{u,p_1}M_{y_u}\Big),\\
m_{\tilde{Y}u^*_L\tilde{Y}u_R} &= \frac{1}{\sqrt{2}}\Big(v_dA^*_{y_u}-v_uY_{y_u}\mu\Big),\\
m_{\tilde{Y}u^*_R\tilde{Y}u_R} &= \frac{1}{2}\Big(2\Big(m^2_{Yu}+M^2_{y_u}\Big)+v_d^2Y^2_{y_u}\Big)+\frac{1}{6}g_1^2\Big(-v_d^2+v_u^2\Big).
\end{aligned} \tag{9}$$

In addition to the elements like the MSSM, $m_{\tilde{Y}u^*_R\tilde{u}^*_L}$, M_{y_q,o_1} and the similar terms arising from the F-term potential of the bilinear terms are the special terms, and the B_{My_q,o_1} and similar terms coming from the soft terms, as mentioned in subsection 2.1, are also the special terms. The mass matrices for down-type squarks and the sleptons are similar. We use the following convention

$$Z^{F,\dagger}m^2_{\tilde{f}}Z^F = m^{diag.}_{2,\tilde{f}} \tag{10}$$

for the diagonalization, where $f=\ d,\ u,\ e$, $F=\ D,\ U,\ E$, and Z^F are the rotation matrices.

2.3 The Feynman Rules

With the Lagrangians and mass spectra given above, we can derive all Feynman rules of the sfermion sectors. Due to the extra VLPs, the interactions involving quarks/squarks and leptons/sleptons will be different from the MSSM. We list all the Feynman rules that are different from the MSSM in the Appendix, and just give a few comments here:

1. The tree-level FCNC processes in the fermion sectors. It is well-known that both in the SM and in the MSSM, there is no tree-level FCNC process for quarks and leptons. However, with the VLPs, such processes will emerge. For example, the Feynman rule for the $\bar{d}_i d_j Z_\mu$ vertex is

$$\frac{ie}{\sin 2\Theta_W}\gamma_\mu\Big[-\frac{2}{3}\sin^2\Theta_W\delta_{ij}+\Big(\delta_{ij}-U^{d,*}_{L,j5}U^{d}_{L,i5}\Big)P_L+U^{d,*}_{R,i5}U^{d}_{R,j5}P_R\Big]\,, \tag{11}$$

and that for the $\bar{d}_i d_j h_k$ vertex is

$$\begin{aligned}&-i\frac{1}{\sqrt{2}}\Big[(U^{d,*}_{R,ia}Y_{d,ab}U^{d,*}_{L,jb}Z^H_{k1}+Y_{y_d}U^{d,*}_{L,j5}U^{d,*}_{R,i5}Z^H_{k2})P_L\\&+(U^{d}_{R,ja}Y^{*}_{d,ab}U^{d}_{L,ib}Z^H_{k1}+Y_{y_d}U^{d}_{L,i5}U^{d}_{R,j5}Z^H_{k2})P_R\Big]\,,\end{aligned} \tag{12}$$

where the interaction state subscripts a and b run from 1 to 4. If we set the subscripts $i \neq j$, we can get the tree-level FCNC interations. Generally speaking, such interactions should be much smaller than the other SM interactions.

2. The deviation from unitarity. Accompanying with the tree-lever FCNC interactions, the vertex which involves the rotation matrix will be non-unitarity. For example, the $\bar{u}_i d_j W^-_\mu$ vertex is

$$-\,i\frac{g_2}{\sqrt{2}}\gamma_\mu\Big[U^{d,*}_{L,ja}U^{u}_{L,ia}P_L-U^{u,*}_{R,i5}U^{d}_{R,j5}P_R\Big]. \tag{13}$$

Since the interaction state subscript a runs from 1 to 4, it makes the summation non-unitarity. In the SM, the quark mixings are described by a unitarity CKM matrix

$$V_{\rm CKM}=\sum_{a=1}^{3}U^{d,*}_{L,ja}U^{u}_{L,ia}\,.$$

Such deviation commonly emerges in every interaction listed in the Appendix. Of course, the deviation form the unitarity should be very small. Otherwise, it will be excluded by the current experimental limits. These tree-level FCNC terms of Eqs. (11) and (12), which are called as "tail terms", lead to rich phenomenology for low energy processes [22].

3. The interactions from F-term potential of the bilinear terms. The tree-level FCNC processes and deviations from the unitarity commonly exist in the SUSY particle sector (shown in the Appendix). In addition, from Eq. (8) one can easily find that the mass contents and interactions form F-term potential are also different from the MSSM. For example, in the $\tilde{u}_i\tilde{u}_j h_i$ vertex, there exist the following terms

$$\cdots+6\sqrt{2}\Big(Y^{*}_{u,ba}M_{y_q,a}Z^{U,*}_{j4+b}Z^{U}_{k9}+Y^{*}_{u,ab}M_{y_u,a}Z^{U,*}_{j10}Z^{U}_{kb}\Big)Z^H_{i2}+\cdots\,, \tag{14}$$

which come form the F-term potential, namely the bilinear terms in the superpotential.

3 The Leading Radiative Corrections to Higgs Boson Mass in the MSSMV

As mentioned above, the tree-level FCNC processes and deviationd from the unitarity in the MSSMV should be much smaller, so their radiative corrections can be neglected in most processes. The new terms from the F-term potential of bilinear terms are the first things which should be checked. Their one-loop contributions to the Higgs boson mass can show the dominant difference between the MSSM and the MSSMV. In this Section, for simplicity, we choose only one pair of the VLPs, namely, only one X and one Y for our study. Note that the contribution from X_u and X_q particles will be exactly the same as top quark in format sicne they have the same quantum numbers. In the following we will study the difference between the contributions from X and Y particles. The superpotential containing the bilinear terms is

$$\begin{aligned} W &= \mu \hat{H}_u \hat{H}_d + Y_{x_u} \hat{X}_u \hat{X}_q \hat{H}_u - Y_{y_u} \hat{Y}_u \hat{Y}_q \hat{H}_d \\ &\quad + M_{y_q} \hat{X}_q \hat{Y}_q + M_{y_u} \hat{X}_u \hat{Y}_u \end{aligned} \tag{15}$$

In this simplified model, for the quark/squark sector there are two quarks (labeled as $m_i, \ \ i = 1, \ 2$) and four squarks (labeled as $m_{\tilde{i}}, \ \ i = \ 1, \ 2, \ 3, \ 4$). The mass matrices of Eqs. (6) and (8) are simplified as well.

The radiative corrections to Higgs boson mass have been studied in Ref. [16] which used the effective potential method. A more detailed study should be on-shell renomalization. In this work we follow Ref. [30], using on-shell renomalization to obtain the analytical results of the leading-order radiative corrections to the Higgs boson mass, which are

$$\begin{aligned} m^2_{h,H} &= \frac{m_A^2 + m_Z^2 + w + \sigma}{2} \mp \left[\frac{(m_A^2 + m_Z^2)^2 + (w-\sigma)^2}{4} - m_A^2 m_Z^2 \cos^2 2\beta \right. \\ &+ \left. \frac{(w-\sigma)\cos 2\beta}{2}(m_A^2 - m_Z^2) - \frac{\lambda \sin 2\beta}{2}(m_A^2 + m_Z^2) + \frac{\lambda^2}{4} \right]^{\frac{1}{2}}, \end{aligned} \tag{16}$$

where h is the SM-like Higgs, and H is the CP-even heavy Higgs in the MSSMV. In this work, we concentrate on the radiative corrections to the SM-like Higgs boson mass. $\omega, \ \lambda, \ \sigma$ are obtained from the self-energy diagrams for the Higgs and gauge bosons. Neglecting the tree-level FCNC processes and deviations from unitarity, we get the leading terms of $\omega, \ \lambda, \ \sigma$ in the MSSMV

$$\begin{aligned} \omega &= \frac{N_c G_F v^2}{4\sqrt{2}\pi^2} \left\{ 2Y_{x_u}^2 \sum_{i,j} U^{u\dagger}_{L,1i} U^u_{R,1j} U^{u\dagger}_{L,1i} U^u_{R,1j} m_i m_j B_0(k^2, m_i^2, m_j^2) \right. \\ &+ Y_{x_u}^2 \left[\frac{1}{2} Y_{x_u}^2 v_u^2 (X_{1111} + X_{2222}) + M_{y_q}^2 X_{2323} + M_{y_u}^2 X_{1414} \right] \\ &+ 2Y_{x_u}^2 A_{x_u} \left[\frac{1}{\sqrt{2}} Y_{x_u} v_u (X_{2122} + X_{2111}) + M_{y_q} X_{2123} + M_{y_u} X_{2114} \right] \\ &+ Y_{x_u}^2 \left[A_{x_u}^2 X_{2121} + \sqrt{2} Y_{x_u} v_u (M_{y_q} X_{2322} + M_{y_u} X_{1411}) \right] \\ &+ \left. \left[Y_{y_u}^2 \mu^2 X_{4343} - 2 Y_{x_u} Y_{y_u} \mu (M_{y_q} X_{4323} - M_{y_u} X_{4314}) \right] \right\}, \end{aligned} \tag{17}$$

$$\begin{aligned} \sigma &= \frac{N_c G_F v^2}{4\sqrt{2}\pi^2} \left\{ 2Y_{y_u}^2 \sum_{i,j} U^{u\dagger}_{L,2i} U^u_{R,2j} U^{u\dagger}_{L,2i} U^u_{R,2j} m_i m_j B_0(k^2, m_i^2, m_j^2) \right. \\ &+ Y_{y_u}^2 \left[\frac{1}{2} Y_{y_u}^2 v_d^2 (X_{3333} + X_{4444}) + M_{y_u}^2 X_{2323} + M_{y_q}^2 X_{1414} \right] \\ &+ 2Y_{y_u}^2 A_{y_u} \left[\frac{1}{\sqrt{2}} Y_{y_u} v_d (X_{4344} + X_{4333}) + M_{y_u} X_{4323} + M_{y_q} X_{4314} \right] \\ &+ Y_{y_u}^2 \left[A_{y_u}^2 X_{4343} + \sqrt{2} Y_{y_u} v_d (M_{y_u} X_{2333} + M_{y_q} X_{1444}) \right] \\ &+ \left. \left[Y_{x_u}^2 \mu^2 X_{2121} - 2 Y_{x_u} Y_{y_u} \mu (M_{y_u} X_{2123} + M_{yq} X_{2114}) \right] \right\}, \end{aligned} \tag{18}$$

$$
\begin{aligned}
\lambda &= \frac{N_C G_F v^2}{2\sqrt{2}\pi^2}\Big\{\mu\Big[\frac{1}{\sqrt{2}}Y_{x_u}^3 v_u(X_{2122}+X_{2111})+\frac{1}{\sqrt{2}}Y_{y_u}^3 v_d(X_{4344}+X_{4333})\Big] \\
&+ \mu\Big[Y_{x_u}^2(M_{y_q}X_{2123}+M_{y_u}X_{2114})+Y_{y_u}^2(M_{y_u}X_{4323}+M_{y_q}X_{4314})\Big] \\
&+ \mu(Y_{x_u}^2 A_{x_u}X_{2121}+Y_{y_u}^2 A_{y_u}X_{4343}) \\
&- Y_{x_u}Y_{y_u}\Big[\frac{1}{\sqrt{2}}Y_{x_u}v_u(M_{y_u}X_{2322}+M_{y_q}X_{1411})+\frac{1}{\sqrt{2}}Y_{y_u}v_d(M_{y_q}X_{2333}+M_{y_u}X_{1444})\Big] \\
&- Y_{x_u}Y_{y_u}\Big[A_{x_u}(M_{y_u}X_{2123}+M_{y_q}X_{2114})+A_{y_u}(M_{y_q}X_{4323}+M_{y_u}X_{4314})\Big] \\
&- Y_{x_u}Y_{y_u}M_{y_q}M_{y_u}(X_{2233}+X_{1144})\Big\}, \qquad (19)
\end{aligned}
$$

where X_{klmn} is defined as

$$
X_{klmn} \equiv \sum_{\tilde{i},\tilde{j}} Z^U_{\tilde{k}\tilde{i}} Z^{UT}_{\tilde{i}\tilde{l}} Z^U_{\tilde{m}\tilde{j}} Z^{UT}_{\tilde{j}\tilde{n}} \times B_0(\mu^2, m^2_{\tilde{i}}, m^2_{\tilde{j}}) \ , \qquad (20)
$$

which come from the summation of the propagators in the loop. The convergent loop function is

$$
B_0(\mu^2,x^2,y^2) = \begin{cases} \log\frac{\mu^2}{y^2}+1+\frac{x^2/y^2}{1-x^2/y^2}\log\frac{x^2}{y^2} & \text{if } x\neq y, \\ \log\frac{\mu^2}{x^2}, & \text{if } x=y \end{cases} \ . \qquad (21)
$$

From the above formulae of ω, λ, σ, the first terms of Eqs. (17), (18) and (19) in the brackets come from the quark loops and the rest contributions come from the squark loops.

As a double check, we find that our results can be reduced to the previous results for example in Refs. [25, 26], if we ignore the bilinear terms. Also, the most important feature of this work is that we notice the bilinear-term coefficients' contributions to the Feynman rules, and then to the Higgs boson mass corrections. Thus, we need to study it and compare the results here.

With the above formulae, we can divide the radiative corrections to the Higgs boson mass into three cases to study.

- Case without bilinear terms

In order to study the physics of the bilinear terms, first we should learn what will happen if we do not have bilinear terms. From superpotential in Eq. (15) and the mass matrices in Eqs. (6) and (8), we can see that if we set $M_{y_q}=0$ and $M_{y_u}=0$, X-type quarks/squarks and Y-type quarks will form separate sectors. Their contributions to ω, λ, σ can be divided into ω_x, λ_x, σ_x and ω_y, λ_y, σ_y, which are given by

$$
\begin{aligned}
\omega_x &= -\frac{N_c G_F m_x^4}{\sqrt{2}\pi^2\sin^2\beta}\Big[\log\frac{m_{\tilde{x}_1}m_{\tilde{x}_2}}{m_x^2}+\frac{A_x(A_x-\mu\cot\beta)}{m^2_{\tilde{x}_1}-m^2_{\tilde{x}_2}}\log\frac{m^2_{\tilde{x}_1}}{m^2_{\tilde{x}_2}} \\
&+\frac{A_x^2(A_x-\mu\cot\beta)^2}{(m^2_{\tilde{x}_1}-m^2_{\tilde{x}_2})^2}(1-\frac{m^2_{\tilde{x}_1}+m^2_{\tilde{x}_2}}{m^2_{\tilde{x}_1}-m^2_{\tilde{x}_2}}\log\frac{m_{\tilde{x}_1}}{m_{\tilde{x}_2}})\Big] \ , \qquad (22) \\
\omega_y &= -\frac{N_c G_F m_y^4}{\sqrt{2}\pi^2\cos^2\beta}\Big[\frac{\mu^2(A_y-\mu\tan\beta)^2}{(m^2_{\tilde{y}_1}-m^2_{\tilde{y}_2})^2}(1-\frac{m^2_{\tilde{y}_1}+m^2_{\tilde{y}_2}}{m^2_{\tilde{y}_1}-m^2_{\tilde{y}_2}}\log\frac{m_{\tilde{y}_1}}{m_{\tilde{y}_2}})\Big] \ , \qquad (23)
\end{aligned}
$$

$$\lambda_x = -\frac{N_c G_F m_x^4}{\sqrt{2}\pi^2 \sin^2\beta}\left[\frac{\mu(A_x-\mu\cot\beta)}{m_{\tilde{x}_1}^2-m_{\tilde{x}_2}^2}\log\frac{m_{\tilde{x}_1}^2}{m_{\tilde{x}_2}^2} + \frac{2\mu A_x(A_x-\mu\cot\beta)^2}{(m_{\tilde{x}_1}^2-m_{\tilde{x}_2}^2)^2}(1-\frac{m_{\tilde{x}_1}^2+m_{\tilde{x}_2}^2}{m_{\tilde{x}_1}^2-m_{\tilde{x}_2}^2}\log\frac{m_{\tilde{x}_1}}{m_{\tilde{x}_2}})\right], \quad (24)$$

$$\lambda_y = -\frac{N_c G_F m_y^4}{\sqrt{2}\pi^2 \cos^2\beta}\left[\frac{\mu(A_y-\mu\tan\beta)}{m_{\tilde{y}_1}^2-m_{\tilde{y}_2}^2}\log\frac{m_{\tilde{y}_1}^2}{m_{\tilde{y}_2}^2} + \frac{2\mu A_y(A_y-\mu\tan\beta)^2}{(m_{\tilde{y}_1}^2-m_{\tilde{y}_2}^2)^2}(1-\frac{m_{\tilde{y}_1}^2+m_{\tilde{y}_2}^2}{m_{\tilde{y}_1}^2-m_{\tilde{y}_2}^2}\log\frac{m_{\tilde{y}_1}}{m_{\tilde{y}_2}})\right], \quad (25)$$

$$\sigma_x = -\frac{N_c G_F m_x^4}{\sqrt{2}\pi^2 \sin^2\beta}\left[\frac{\mu^2(A_x-\mu\cot\beta)^2}{(m_{\tilde{x}_1}^2-m_{\tilde{x}_2}^2)^2}(1-\frac{m_{\tilde{x}_1}^2+m_{\tilde{x}_2}^2}{m_{\tilde{x}_1}^2-m_{\tilde{x}_2}^2}\log\frac{m_{\tilde{x}_1}}{m_{\tilde{x}_2}})\right], \quad (26)$$

$$\sigma_y = -\frac{N_c G_F m_y^4}{\sqrt{2}\pi^2 \cos^2\beta}\left[\log\frac{m_{\tilde{y}_1}m_{\tilde{y}_2}}{m_y^2} + \frac{A_y(A_y-\mu\tan\beta)}{m_{\tilde{y}_1}^2-m_{\tilde{y}_2}^2}\log\frac{m_{\tilde{y}_1}^2}{m_{\tilde{y}_2}^2} + \frac{A_y^2(A_y-\mu\tan\beta)^2}{(m_{\tilde{y}_1}^2-m_{\tilde{y}_2}^2)^2}(1-\frac{m_{\tilde{y}_1}^2+m_{\tilde{y}_2}^2}{m_{\tilde{y}_1}^2-m_{\tilde{y}_2}^2}\log\frac{m_{\tilde{y}_1}}{m_{\tilde{y}_2}})\right]. \quad (27)$$

Note that, in this case the vector-like quark masses are

$$m_x = \frac{Y_x}{\sqrt{2}}v_u, \quad m_y = \frac{Y_y}{\sqrt{2}}v_d\,, \quad (28)$$

which have been used in the formulae.

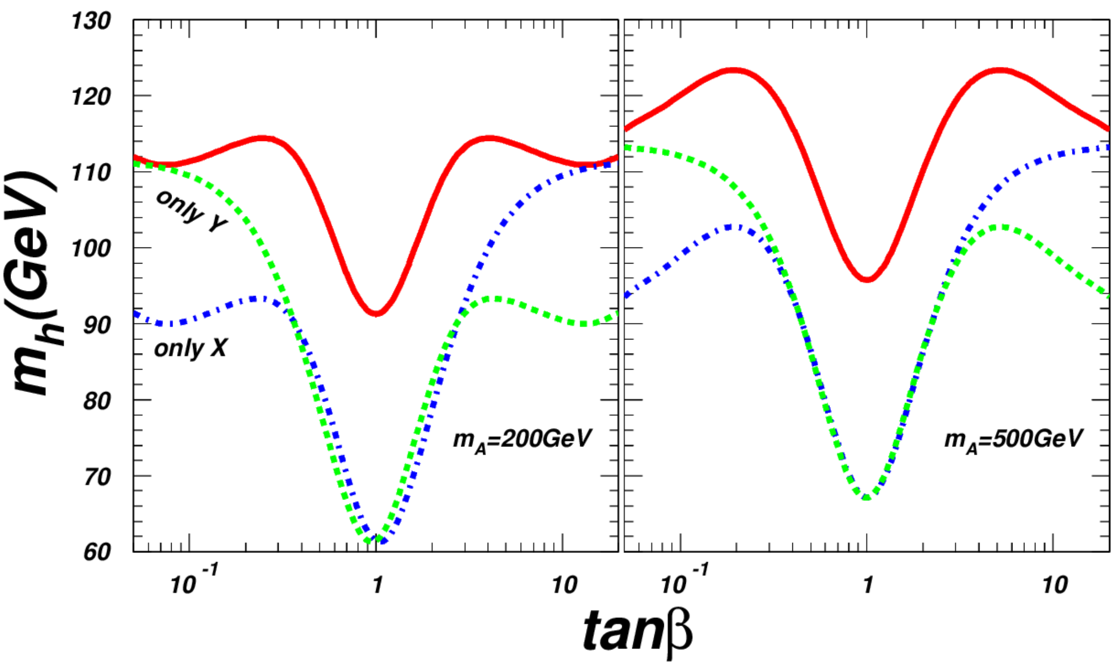

Figure 1: The Higgs boson mass m_h versus $\tan\beta$ with different M_A. The solid, dot dash and dash lines denotes the total contribution, the contributions solely from X-type VLPs and Y-type VLPs, respectively.

As we discussed above, ω_x, λ_x, σ_x are exactly same as the leading contributions of top quark and squark in the MSSM in form. Furthermore, from Eq. (16) and the superpotential in Eq. (15), we get that if setting all the corresponding input parameters the same, under $\tan\beta \leftrightarrow \cot\beta$, the contributions to the radiative correction from X-type VLPs and Y-type VLPs are symmetric. The point is that if we neglect the Yukawa couplings of the third generation especially top quarks/squarks, there is a symmetry between H_d and H_u. However, $\tan\beta$ cannot be smaller than about 2 for consistency in the supersymmetric SMs.

To illustrate the symmetry more clearly, we plot the corrected Higgs mass m_h versus the $\tan\beta$ with different input M_A in Fig. 1. The $\tan\beta$ axis is in logarithmic coordinate. We can see that both panels are mirror symmetric on the axis $\tan\beta = 1$. In our numerical calculations all other parameters are taken as

$$\mu = 200 \text{ GeV},\ m_x = m_y = 200 \text{ GeV},\ m_{\tilde{x}_1} = m_{\tilde{x}_1} = 450 \text{ GeV},\ m_{\tilde{x}_2} = m_{\tilde{x}_2} = 550 \text{ GeV},\ A_x = A_y = 1500 \text{ GeV},$$

for the left panel and

$$\mu = 50 \text{ GeV},\ m_x = m_y = 200 \text{ GeV},\ m_{\tilde{x}_1} = m_{\tilde{x}_1} = 450 \text{ GeV},\ m_{\tilde{x}_2} = m_{\tilde{x}_2} = 550 \text{ GeV},\ A_x = A_y = 1000 \text{ GeV},$$

for the right panel.

Following the convention, we define variables

$$\begin{aligned} X_x &\equiv A_x - \mu\cot\beta\,, \\ X_y &\equiv A_y - \mu\tan\beta \end{aligned} \tag{29}$$

for the next step. It is also clear that if we do the transformation:

$$\omega_x \leftrightarrow \sigma_y,\ \sigma_x \leftrightarrow \omega_y,\ \lambda_x \leftrightarrow \lambda_y,\ X_x \leftrightarrow X_y, \tag{30}$$

the contributions from X and Y particles are symmetric, as displayed in Fig. 2.

Another very important feature we find is the contribution of X-type VLPs is dominant in case of large $\tan\beta$ while the contribution of Y-type VLPs is dominant in case of large $\cot\beta$. This is conflict with our intuitive judgement, because the Yukawa coupling of X-type quark is $\cot\beta$ enhanced and Y-type quark is $\tan\beta$ enhanced. However, one can confirm this conclusion after careful checking by comparing Eq. (23) with Eq. (27). The reason is that the enhanced terms of ω, σ, λ canceled each other, leaving an enhancement trend that is beyond simple intuition. For example, in case of large $\cot\beta$, the enhanced ω_x, σ_x in first term of Eq. (16) are cancelled by the second root term, making the radiative correction dominantly from ω_y, λ_y, σ_y.

Because the radiative corrections are symmetric on the interchange of $\tan\beta$ and $\cot\beta$ if we neglect the third generation, we can image that the sole corrections from the X-type quarks and those from Y-type quarks will be exactly the same by changing $\tan\beta$ to its inverse. This is clearly shown in Fig. 2. Fig. 2 shows m_h versus m_A and X_x or X_y individually. In the left panel, we set $X_x = 0$ and 600 GeV, $\tan\beta = 20$ and 2, and vary M_A, while in the right panel, we vary X_x or X_y at different M_A. From the left panel, we can also see that when M_A increases, the heavy Higgs particles will decouple at the EW scale and then there is one SM like Higgs with mass about 100 GeV, but the SUSY radiative corrections can lift the Higgs boson mass. The right panel shows the effects of the mixings among squarks. Because X_x and X_y determine the mixings between $\tilde{x}_L$, $\tilde{x}_R$ and $\tilde{y}_L$, $\tilde{y}_R$, there is no mixing in squark sector when $X_{x,y} = 0$, and then the radiative corrections only depend on the mass splittings between quarks and squarks, namely the first terms of ω_x and σ_y. An appropriate X_x or X_y can give large logarithmic terms $\log(m^2_{\tilde{x}_1}/m^2_{\tilde{x}_2})$ or $\log(m^2_{\tilde{y}_1}/m^2_{\tilde{y}_2})$, which will enhance the radiative corrections.

To calculate the Higgs boson mass more precisely, we add the top quark/squark contributions, and

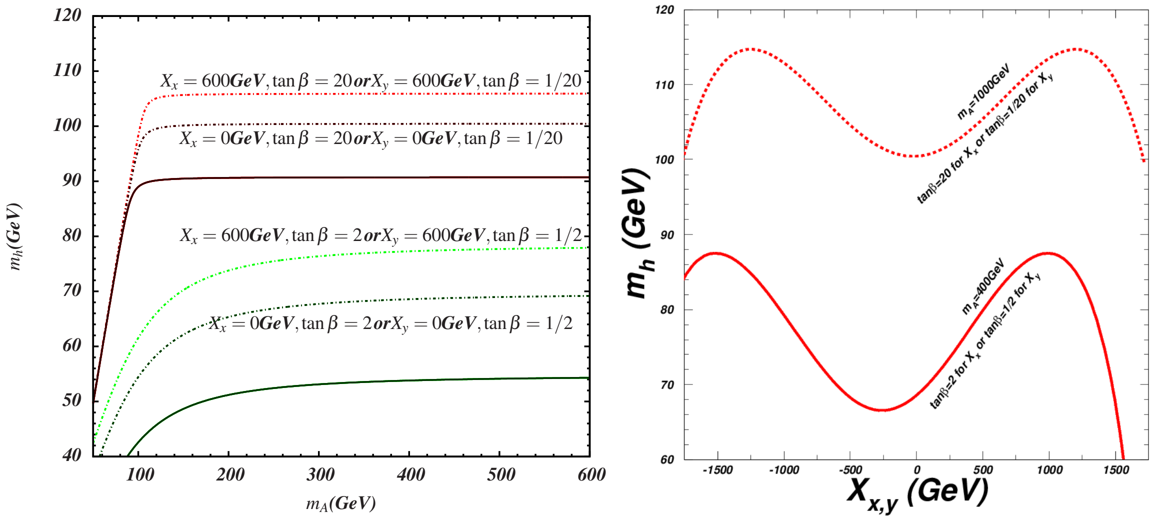

Figure 2: The Higgs boson mass m_h versus m_A and X_x or X_y, The trend of X-type quark is the same as the top quark. The result of Y-type quark is exactly the same as X-type quark by changing $\tan\beta$ to $1/\tan\beta$.

the analytical one-loop contributions to the Higgs boson from the top quarks/squarks are

$$\omega_t = \omega_x(m_x \to m_t, m_{\tilde{x}_1} \to m_{\tilde{t}_1}, m_{\tilde{x}_2} \to m_{\tilde{t}_2}, A_x \to A_t), \quad (31)$$

$$\lambda_t = \lambda_x(m_x \to m_t, m_{\tilde{x}_1} \to m_{\tilde{t}_1}, m_{\tilde{x}_2} \to m_{\tilde{t}_2}, A_x \to A_t), \quad (32)$$

$$\sigma_t = \sigma_x(m_x \to m_t, m_{\tilde{x}_1} \to m_{\tilde{t}_1}, m_{\tilde{x}_2} \to m_{\tilde{t}_2}, A_x \to A_t). \quad (33)$$

Thus the complete ω, λ, σ should be

$$\omega = \omega_x + \omega_y + \omega_t, \quad (34)$$

$$\lambda = \lambda_x + \lambda_y + \lambda_t, \quad (35)$$

$$\sigma = \sigma_x + \sigma_y + \sigma_t, \quad (36)$$

and we choose the same input parameters as in Fig. 2, except $\tan\beta = 10$. For $A_T = 2000$ GeV, $m_{\tilde{t}_1} = 950$ GeV, and $m_{\tilde{t}_2} = 1050$ GeV, we present the Higgs boson mass m_h versus m_A in Fig. 3.

In Fig. 3, the red solid line represents the tree-level Higgs mass, the green dashed line represents the Higgs mass with the VLPs' contributions, and the blue dashed line represents the Higgs mass with both the VLPs' contributions and the third generation's contributions. Clearly, the corrections from VLPs is positive, but not enough for a 125 GeV Higgs. After including the corrections from the third generation, realizing a 125 GeV Higgs boson is not difficult in this parameter space.

- Case with the (partial) decoupling limit

In a supersymmetric theory, the masses of fermion(s) and sfermion(s) in a chiral superfield are degenerated. The soft breaking terms are added to the Lagrangian to split the spectra of the fermions and sfermions in the phenomenological models. Thus, there is a limit with vanishing super-trace, *i.e.*, $\text{Str}M^2 = 0$. We find this limit would be a very special situation to the MSSMV, since the bilinear term coefficients will be more prominent.

If soft breaking parameters in the quark/squark sector are all ignored, we only have the supersymmetric lagrangian generated from the superpotential in Eq. (15) for quarks and squarks. For example, the

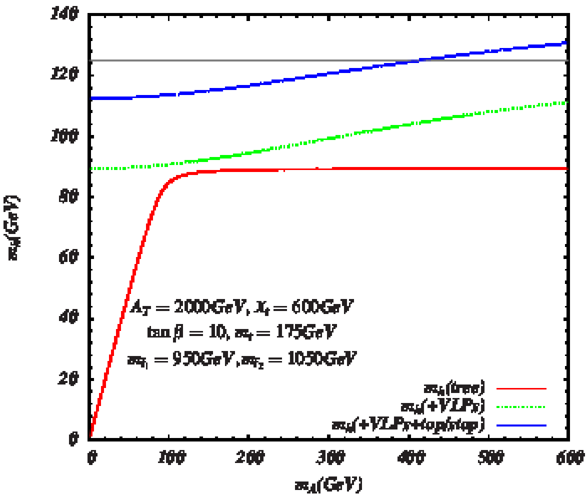

Figure 3: The Higgs boson mass m_h versus m_A to reflect the mass. The numerical value of the gray line is 125 GeV.

mass matrix of quarks is

$$\begin{pmatrix} \frac{1}{\sqrt{2}} Y_x v_u & M_{y_q} \\ M_{y_u} & \frac{1}{\sqrt{2}} Y_y v_d \end{pmatrix}. \tag{37}$$

So the X-type quarks and Y-type quarks can be mixed. The mass matrix for squarks (dropping all the soft term of Eq. (8)) is

$$\begin{pmatrix} (\frac{v_u}{\sqrt{2}} Y_x)^2 + M_{y_q}^2 & 0 & 0 & M_{y_u} \frac{v_u}{\sqrt{2}} Y_x + M_{y_q} \frac{v_d}{\sqrt{2}} Y_y \\ 0 & (\frac{v_u}{\sqrt{2}} Y_x)^2 + M_{y_u}^2 & M_{y_q} \frac{v_u}{\sqrt{2}} Y_x + M_{y_u} \frac{v_d}{\sqrt{2}} Y_y & 0 \\ 0 & M_{y_q} \frac{v_u}{\sqrt{2}} Y_x + M_{y_u} \frac{v_d}{\sqrt{2}} Y_y & (\frac{v_d}{\sqrt{2}} Y_y)^2 + M_{y_q}^2 & 0 \\ M_{y_u} \frac{v_u}{\sqrt{2}} Y_x + M_{y_q} \frac{v_d}{\sqrt{2}} Y_y & 0 & 0 & (\frac{v_d}{\sqrt{2}} Y_y)^2 + M_{y_u}^2 \end{pmatrix}. \tag{38}$$

Although there are four squarks in the spectra, they can be divided into two pairs with degenerated masses. Futhermore, one can check that these two masses are also degenerated with the masses of quarks listed Eq. (37), which is just required by a supersymmetric theory because the four squarks are the super partners of the two quarks.

To test this supersymmetic limit, we choose $g_1 = g_2 = 0$ to remove gauge interactions. We take $M_{y_q} = M_{y_u} = M_V = 1000$ GeV, $M_A = 300$ GeV, $\tan\beta = 5$, and the mass of tree-level Higgs is 83.56 GeV. And then we scan the Yukawa couplings Y_x, Y_y randomly in the range of $(0, \ \ 2)$ and the other soft paramters (together with μ)

$$A_x, \ A_y, \ \sqrt{B_{M_{y_q}} M_{y_q}}, \ \sqrt{B_{M_{y_u}} M_{y_u}},$$

randomly in the range of $(-E_S, +E_S)$ with the parameter E_S denoting the EW energy scale and varing randomly in the range of $(0 \text{ GeV}, \ \ 1000 \text{ GeV})$. The radiative masses of the SM-like Higgs boson versus the EW energy scale are shown in Fig. 4. In Fig. 4, we can see an interesting feature of the MSSMV that the radiative corrections decrease to zero as E_S decreases to zero, and this trend is independent of the billinear parameters M_{y_q} and M_{y_u}. The reason is that fermions and sfermions cancel each other in a supersymmetric theory.

Now let us pay more attention to understand the decoupling limit in the MSSMV. If M_{y_q}, $M_{y_u} \gg E_S$,

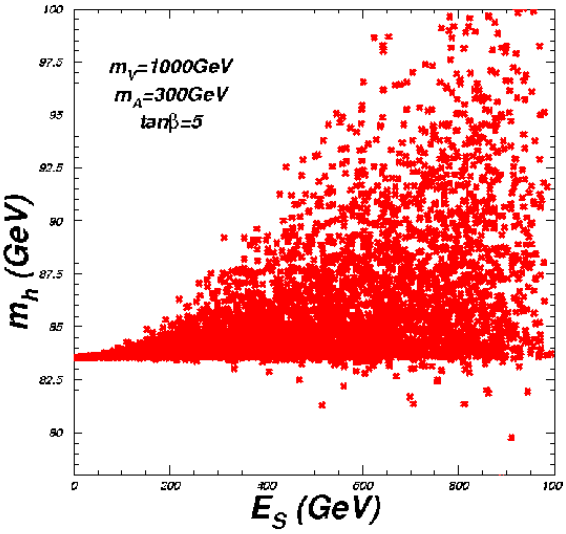

Figure 4: The Higgs mass m_h versus EW energy scale E_S in case of $M_A = 300$ GeV, $\tan\beta = 5$ and $M_{y_q} = M_{y_u} = M_V = 1000$ GeV. All the other soft parameters are scaned randomly in the range $(-E_S, E_S)$. The tree-level SM-like Higgs mass is 83.56 GeV.

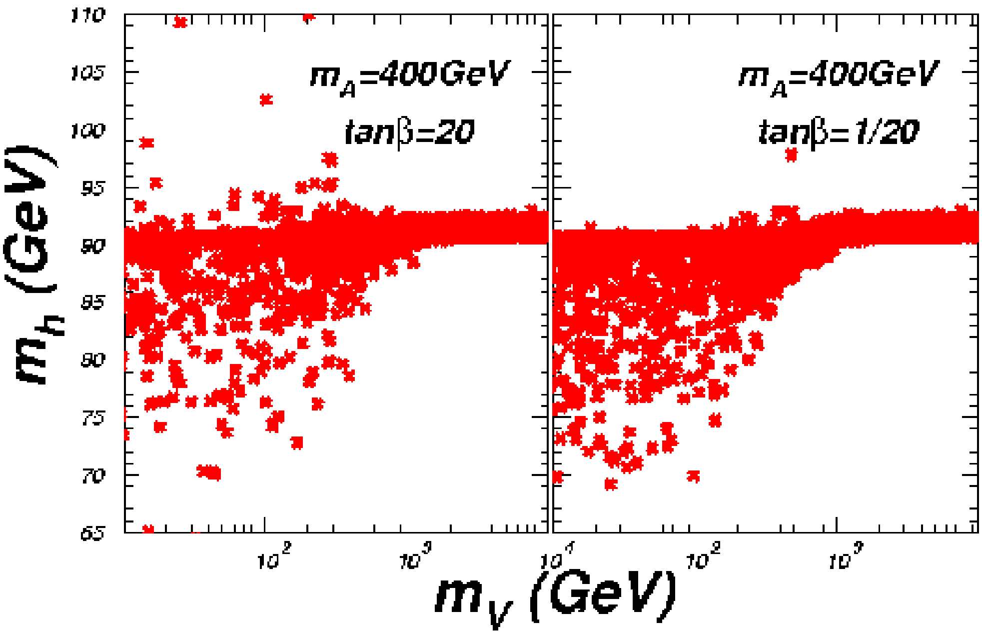

Figure 5: The Higgs mass m_h versus VLP input $M_{y_q} = M_{y_u} = M_V$, in case of $M_A = 400$ GeV, $\tan\beta = 20, 1/20$ and $E_S = 1000$ GeV . All the other soft parameters are scaned randomly in the range $(-E_S, E_S)$. The tree-level SM-like Higgs mass is 83.56 GeV.

the model will recover supersymmetry, and then the effects of VLPs will decouple from the EW energy scale, namely, the radiative corrections to Higgs boson mass will be zero, as demonstrated in Fig. 5.

In Fig. 5, we choose $E_S = 1000$ GeV, $M_A = 400$ GeV, and scan $M_{y_q} = M_{y_u} = M_V$ randomly from 0 GeV to 10 TeV, μ and all the soft paramters in squark sector randomly in the range of $(-E_S,\ E_S)$ with g_1 and g_2 from the SM inputs. Note that the symmetry between $\tan\beta \leftrightarrow \cot\beta$ still remains. We set $\tan\beta = 20$ (left panel) and $\tan\beta = 1/20$ (right panel) for demonstration. From Fig. 5, we can see that the radiative corrections to the Higgs boson mass become a very small value as the M_V increases up to be much heavier than 1 TeV. Thus, the VLPs decouple from the EW energy scale. The decoupling effects can also be seen in Refs. [25, 16]. As the masses of VLPs increase, the splittings between the quarks and squarks as well as the splitings among squarks become more and more negligible. Namely, the term

$$\log \frac{M_S^2 + M_V^2}{M_V^2} \tag{39}$$

approaches to zero, and then the VLPs decouple.

From the above two cases, we conclude that

1. The corrections to the Higgs boson mass in the MSSMV depend on the splitting between quarks and squarks and the splitting among squarks. The soft terms break supersymmetry explicitly, leading to the splitting of the mass spectra.
2. The heavy VLPs can suppress the splitting of the mass spectra. Because there exists the decoupling limit, the heavy VLP effects decouple from the EW energy scale.

- A partial decoupling effect

Now we turn to the case that one VLP input M_{y_q} is at the EW energy scale, but the other one M_{y_u} is free. We find that there exists the decoupling effect as well. Let us take

$$M_{y_u} \gg M_{y_q} \quad , \tag{40}$$

easily we would get one light VLP quark and one heagy VLP quark. So there exist two light squarks and two heavy squarks, and there can be large splittings between quarks and squarks. However, the effects of these large splittings can be suppressed by the heavy particles, the corrections from VLPs including the light and heavy ones decouple at the EW energy scale.

To show this effect, we choose $M_A = 400$ GeV, $\tan\beta = 5$ and $M_{y_q} = 500$ GeV, and scan M_{y_u} in the range of $(0\ \text{GeV},\ \ 100\ \text{TeV})$. μ and all the soft parameters in squark sector vary randomly in the range of $(-1000\ \text{GeV},\ 1000\ \text{GeV})$. The radiative corrections to the Higgs boson mass are given in Fig. 6. We can see that as M_{y_u} increases (bigger than M_{y_q}), the virtual effects of VLPs on Higgs mass become smaller and smaller. Finally, the VLP effects decouple from the EW energy scale, though there are still light quarks and squarks that are around the EW energy scale.

Such suppression can be understood in the similar way as the decoupling limit mentioned above. The splitting between quarks and squarks, and splitting between squarks are still suppressed by the heavy VLPs, so the partial decoupling limits still exist. In fact, after we integrate out $\hat{X}_q$ and $\hat{Y}_q$, we get

$$W \quad \supset \quad \frac{Y_{x_u} Y_{y_u} \hat{X}_u \hat{Y}_u \hat{H}_u \hat{H}_d}{M_{y_q}} \,, \tag{41}$$

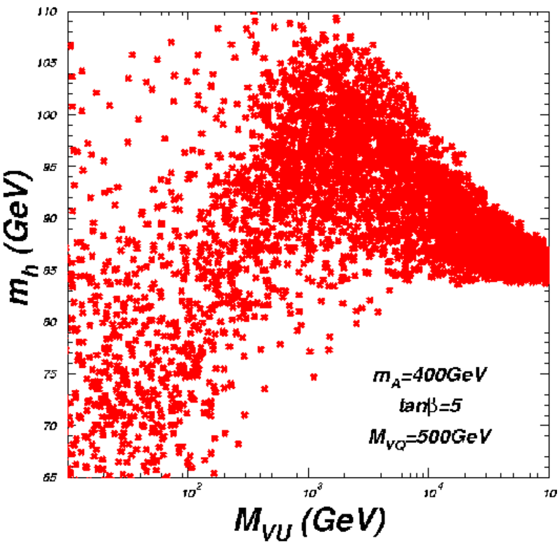

Figure 6: The radiative Higgs boson mass m_h versus VLP input M_{y_u} in case of $M_A = 400$ GeV, $\tan\beta = 5$, $M_{y_q} = 500$ GeV and $E_S = 1000$ GeV. All the other soft parameters are scaned randomly in the range $(-E_S,\ E_S)$. The tree-level SM-like Higgs mass is 83.83 GeV.

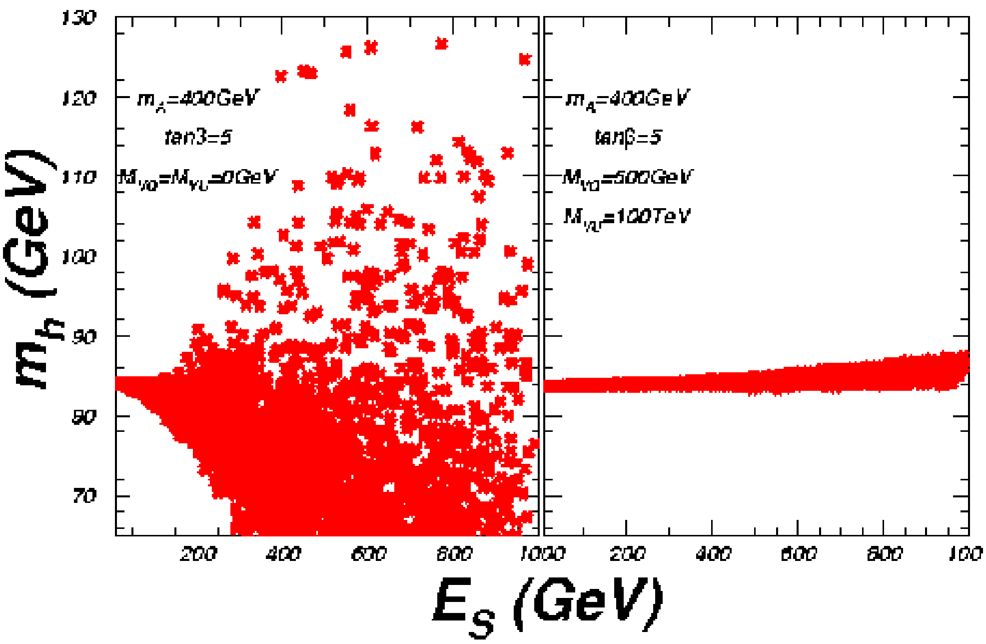

Figure 7: The Higgs mass m_h versus the EW energy scale E_S in case of $M_A = 400$GeV, $\tan\beta = 5$, $M_{y_q} = 500$GeV, and $M_{y_u} = 100$TeV. All the other soft parameters are scanned randomly in the range $(-E_S,\ E_S)$. The tree-level SM-like Higgs mass is 83.83 GeV.

which will be decoupled for very heavy M_{y_q}.

At the end of this Section, we compare the Higgs mass in the cases with and without the bilinear terms. The numerical results are shown in Fig. 7. The left panel shows the results without the bilinear terms (corresponding to the first case), while right panel shows the results with bilinear terms $M_{y_q} = 500$ GeV, $M_{y_u} = 100$ TeV. We can see that the mass of Higgs boson mass can be enhanced in the first case. However, the virtual effects of VLPs are much smaller in case of heavy partners existing. Two benchmark points are presented in Table 2. Note that X-type particle just like the top quark except its bilinear terms

(GeV)	$m_{q_1}(m_x)$	$m_{q_2}(m_y)$	$m_{\tilde{q}_1}(m_{\tilde{x}_1})$	$m_{\tilde{q}_2}(m_{\tilde{x}_2})$	$m_{\tilde{q}_3}(m_{\tilde{y}_1})$	$m_{\tilde{q}_4}(m_{\tilde{y}_2})$	m_h
Without billinear terms	48	240	102	373	444	690	126.2
One heavy billinear terms	500	100000	153	827	100001	100003	84.2

Table 2: The benchmark points of particle spectra with and without heavy VLPs for $\tan\beta = 5$. The tree-level SM-like Higgs mass is 83.83 GeV.

for mass source, but if there is a heavy VLP parter of this particle, their corrections to Higgs mass will be negligible. The reason for this can also be understood from the Feynman rules of hq_iq_j and $h\tilde{q}_i\tilde{q}_j$. The couplings between Higgs and two light quarks are also suppressed by the rotation matrices, leading the radiative results of loops are negligible. On the other hand, if we want the radiative corrections from the X-type VLP quarks and squarks to enhance the tree-level Higgs mass to 125 GeV, the Y-type VLP partner will be strictly constrained. The detail study of such phenomenology is beyond this work.

4 Summary

We proposed the MSSMV, and studied the particle spectra and Feynman rules in the quark/lepton and squark/slepton sectors. Due to the participation of bilinear terms, we found three different points compared to the Feynman rules in the MSSM

1. The tree-level FCNC processes in the quark/lepton sectors.
2. Deviation from unitarity.
3. Interactions from F-term potential of the bilinear terms.

Using these Feynman rules, we studied the analytical one-loop radiative contributions to Higgs mass with one pair of VLPs. We found a very interesting mechanism in the MSSMV. All the effects of VLPs can decouple from the EW energy scale if the bilinear terms are much heavy. And if there are one light bilinear term and one heavy bilinear term, the virtual effects of the light one can be suppressed by the heavy one. This suppression can make the EW phenomenology highly different from the MSSM. Note that in our above study of the radiative corrections to Higgs mass, we ignored the experimental limits on the input parameters such as $\tan\beta$, M_S, etc. A complete study will be given elsewhere.

Acknowledgment

The work of T.L. is supported by the Natural Science Foundation of China under grant numbers 11135003, 11275246, and 11475238. The work of W. Y. Wang was supported by the Natural Science Foundation of China under grant numbers 11375001, the Ri-Xin Foundation of BJUT and Youth-Talents Foundation of eduction department of Beijing.

Appendix A

We shall list the Feynman rules for the interactions involving VLPs, where all the interaction state summing subscripts run from 1 to 4.

1. Fermion-Higgs Boson

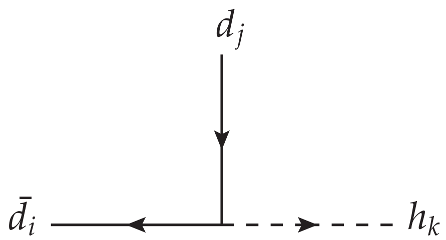

$$-i\frac{1}{\sqrt{2}}\Big[(U^{d,*}_{R,ia}Y_{d,ab}U^{d,*}_{L,jb}Z^H_{k1}+Y_{yd}U^{d,*}_{L,j5}U^{d,*}_{R,i5}Z^H_{k2})P_L$$
$$+(U^d_{R,ja}Y^*_{d,ab}U^d_{L,ib}Z^H_{k1}+Y_{yd}U^d_{L,i5}U^d_{R,j5}Z^H_{k2})P_R\Big]$$

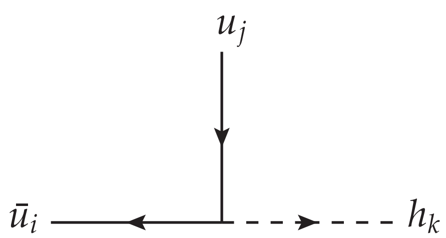

$$-i\frac{1}{\sqrt{2}}\Big[(U^{u,*}_{R,ia}Y_{u,ab}U^{u,*}_{L,jb}Z^H_{k2}+Y_{yu}U^{u,*}_{L,j5}U^{u,*}_{R,i5}Z^H_{k1})P_L$$
$$+(U^u_{R,ja}Y^*_{u,ab}U^u_{L,ib}Z^H_{k2}+Y_{yu}Z^H_{k1}U^u_{L,i5}U^u_{R,j5})P_R\Big]$$

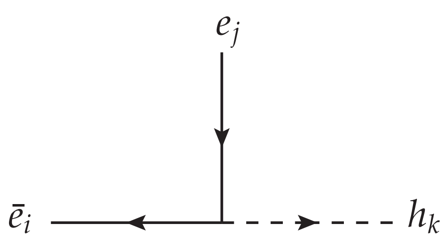

$$-i\frac{1}{\sqrt{2}}\Big[(U^{e,*}_{R,ia}Y_{e,ab}U^{e,*}_{L,jb}Z^H_{k1}+Y_{ye}U^{e,*}_{L,j5}U^{e,*}_{R,i5}Z^H_{k2})P_L$$
$$+(U^e_{R,ja}Y^*_{e,ab}U^e_{L,ib}Z^H_{k1}+Y_{ye}U^e_{L,i5}U^e_{R,j5}Z^H_{k2})P_R\Big]$$

2. Fermion-Gauge Boson

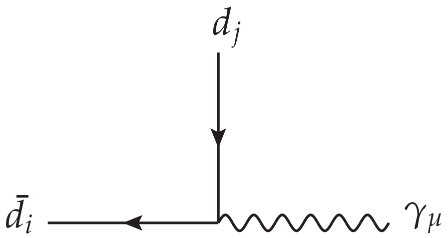

$$-i\frac{1}{3}e\gamma_\mu$$

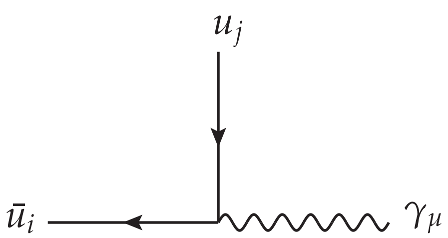

$$i\frac{2}{3}e\gamma_\mu$$

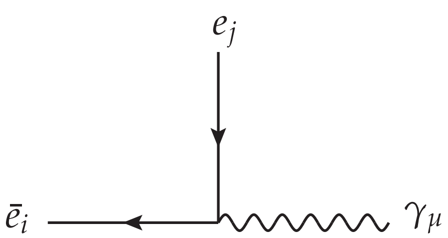

$$-ie\gamma_\mu$$

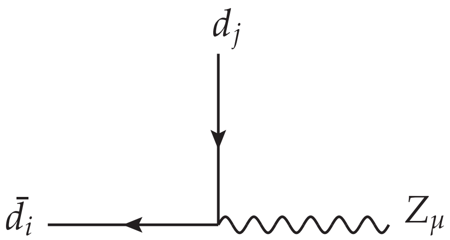

$$\frac{ie}{\sin 2\Theta_W}\gamma_\mu\Big[-\frac{2}{3}\sin^2\Theta_W\delta_{ij}+U^{d,*}_{L,ja}U^{d}_{L,ia}P_L+U^{d,*}_{R,i5}U^{d}_{R,j5}P_R\Big]$$

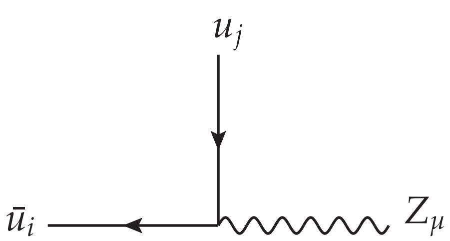

$$\frac{ie}{\sin 2\Theta_W}\gamma_\mu\Big[\frac{4}{3}\sin^2\Theta_W\delta_{ij}-U^{u,*}_{L,ja}U^{u}_{L,ia}P_L-U^{u,*}_{R,i5}U^{u}_{R,j5}P_R\Big]$$

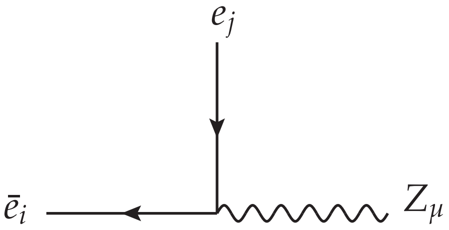

$$\frac{ie}{\sin 2\Theta_W}\gamma_\mu\Big[-2\sin^2\Theta_W\delta_{ij}+U^{e,*}_{L,ja}U^{e}_{L,ia}P_L+U^{e,*}_{R,i5}U^{e}_{R,j5}P_R\Big]$$

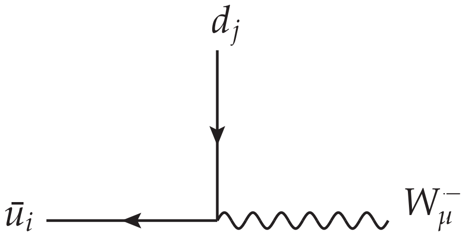

$$-i\frac{g_2}{\sqrt{2}}\gamma_\mu\Big[U^{d,*}_{L,ja}U^{u}_{L,ia}P_L-U^{u,*}_{R,i5}U^{d}_{R,j5}P_R\Big]$$

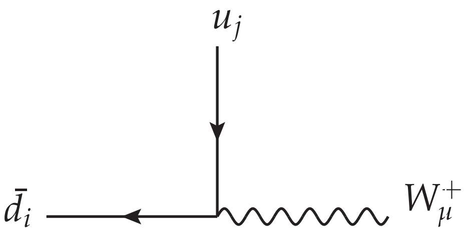

$$-i\frac{g_2}{\sqrt{2}}\gamma_\mu\Big[U^{u,*}_{L,ja}U^{d}_{L,ia}P_L-U^{d,*}_{R,i5}U^{u}_{R,j5}P_R\Big]$$

3. Sfermion-Higgs Boson

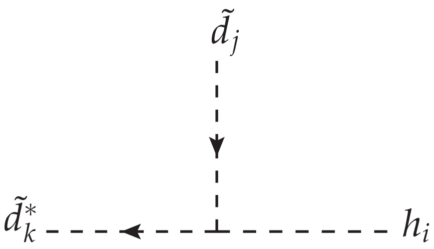

$$
\begin{aligned}
&-\frac{i}{12}\Big\{6\sqrt{2}\Big(A_{Yyd}Z^{D,*}_{j10}Z^{D}_{k9}+A^*_{Yyd}Z^{D,*}_{j9}Z^{D}_{k10}\Big)Z^{H}_{i2}\\
&+6\sqrt{2}\Big(A_{d,ab}Z^{D}_{k4+a}Z^{D,*}_{jb}+A^*_{d,ab}Z^{D,*}_{j4+a}Z^{D}_{kb}\Big)Z^{H}_{i1}\\
&-6\sqrt{2}\Big(\mu^*Z^{D}_{k4+a}Y_{d,ab}Z^{D,*}_{jb}+\mu Z^{D,*}_{j4+a}Y^*_{d,ab}Z^{D}_{kb}\Big)Z^{H}_{i2}\\
&-6\sqrt{2}Y_{yd}\Big(\mu^*Z^{D,*}_{j10}Z^{D}_{k9}+\mu Z^{D,*}_{j9}Z^{D}_{k10}\Big)Z^{H}_{i1}\\
&+6\sqrt{2}\Big(M_{yd,a}Y^*_{d,ab}Z^{D}_{kb}Z^{D,*}_{j10}-M_{yq,a}Y_{d,ba}Z^{D}_{k4+b}Z^{D,*}_{j9}\Big)Z^{H}_{i1}\\
&+6\sqrt{2}\Big(M_{yd,a}Y_{d,ab}Z^{D,*}_{jb}Z^{D}_{k10}-M_{yq,a}Y^*_{d,ba}Z^{D,*}_{j4+b}Z^{D}_{k9}\Big)Z^{H}_{i1}\\
&+6\sqrt{2}Y_{yd}\Big(M_{yd,a}Z^{D,*}_{j4+a}Z^{D}_{k9}-M_{yq,a}Z^{D,*}_{ja}Z^{D}_{k10}\Big)Z^{H}_{i2}\\
&+6\sqrt{2}Y_{yd}\Big(M_{yd,a}Z^{D,*}_{j9}Z^{D}_{k4+a}-M_{yq,a}Z^{D,*}_{j10}Z^{D}_{ka}\Big)Z^{H}_{i2}\\
&+12v_uY^2_{yd}\Big(Z^{D,*}_{j9}Z^{D}_{k9}Z^{H}_{i2}+Z^{D,*}_{j10}Z^{D}_{k10}\Big)Z^{H}_{i2}\\
&+12v_d\Big(Z^{D,*}_{j4+c}Y^*_{d,ca}Y_{d,ba}Z^{D}_{k4+b}+Z^{D,*}_{jb}Y^*_{d,ac}Y_{d,ab}Z^{D}_{kc}\Big)Z^{H}_{i1}\\
&+\Big[\Big(3g_2^2+g_1^2\Big)Z^{D,*}_{j9}Z^{D}_{k9}+2g_1^2Z^{D,*}_{j10}Z^{D}_{k10}\Big]\Big(v_dZ^{H}_{i1}-v_uZ^{H}_{i2}\Big)\\
&-\Big[\Big(3g_2^2+g_1^2\Big)Z^{D,*}_{ja}Z^{D}_{ka}+2g_1^2Z^{D,*}_{j4+a}Z^{D}_{k4+a}\Big]\Big(v_dZ^{H}_{i1}-v_uZ^{H}_{i2}\Big)\Big\}
\end{aligned}
$$

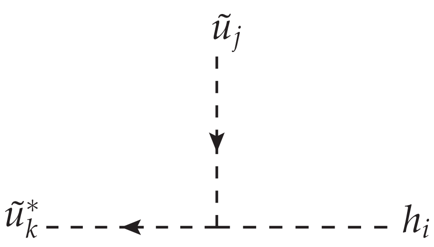

$$
\begin{aligned}
&-\frac{i}{12}\Big\{6\sqrt{2}\Big(A_{Yyu}Z^{U,*}_{j10}Z^{U}_{k9}+6\sqrt{2}A^*_{Yyu}Z^{U,*}_{j9}Z^{U}_{k10}\Big)Z^{H}_{i1}\\
&+6\sqrt{2}\Big(A_{u,ab}Z^{U}_{k4+a}Z^{U,*}_{jb}+A^*_{u,ab}Z^{U,*}_{j4+a}Z^{U}_{kb}\Big)Z^{H}_{i2}\\
&-6\sqrt{2}\Big(\mu^*Y_{u,ab}Z^{U,*}_{jb}Z^{U}_{k4+a}+\mu Y^*_{u,ab}Z^{U,*}_{j4+a}Z^{U}_{kb}\Big)Z^{H}_{i1}\\
&-6\sqrt{2}Y_{yu}\Big(\mu Z^{U,*}_{j9}Z^{U}_{k10}Z^{H}_{i2}+\mu^*Z^{U,*}_{j10}Z^{U}_{k9}\Big)Z^{H}_{i2}\\
&+6\sqrt{2}\Big(M_{yq,a}Y^*_{u,ba}Z^{U,*}_{j4+b}Z^{U}_{k9}+M_{yu,a}Y^*_{u,ab}Z^{U,*}_{j10}Z^{U}_{kb}\Big)Z^{H}_{i2}\\
&+6\sqrt{2}\Big(M_{yq,a}Y_{u,ba}Z^{U}_{k4+b}Z^{U,*}_{j9}+M_{yu,a}Y_{u,ab}Z^{U,*}_{jb}Z^{U}_{k10}\Big)Z^{H}_{i2}\\
&+6\sqrt{2}Y_{yu}\Big(M_{yu,a}Z^{U,*}_{j9}Z^{U}_{k4+a}+M_{yq,a}Z^{U,*}_{j10}Z^{U}_{ka}\Big)Z^{H}_{i1}\\
&+6\sqrt{2}Y_{yu}\Big(M_{yu,a}Z^{U,*}_{j4+a}Z^{U}_{k9}+M_{yq,a}Z^{U,*}_{ja}Z^{U}_{k10}\Big)Z^{H}_{i1}\\
&+12v_dY^2_{yu}\Big(Z^{U,*}_{j9}Z^{U}_{k9}+Z^{U,*}_{j10}Z^{U}_{k10}\Big)Z^{H}_{i1}\\
&+12v_u\Big(Z^{U,*}_{j4+c}Y^*_{u,ca}Y_{u,ba}Z^{U}_{k4+b}+Z^{U,*}_{jb}Y^*_{u,ac}Y_{u,ab}Z^{U}_{kc}\Big)Z^{H}_{i2}\\
&-\Big[\Big(3g_2^2-g_1^2\Big)Z^{U,*}_{j9}Z^{U}_{k9}+4g_1^2Z^{U,*}_{j10}Z^{U}_{k10}\Big]\Big(v_dZ^{H}_{i1}-v_uZ^{H}_{i2}\Big)\\
&+\Big[\Big(3g_2^2-g_1^2\Big)Z^{U,*}_{ja}Z^{U}_{ka}+4g_1^2Z^{U,*}_{j4+a}Z^{U}_{k4+a}\Big]\Big(v_dZ^{H}_{i1}-v_uZ^{H}_{i2}\Big)\Big\}
\end{aligned}
$$

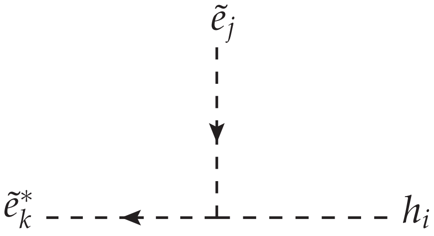

$$\begin{aligned}
&\frac{i}{4}\Big\{-2\sqrt{2}\Big(A_{Yye}Z^{E,*}_{j10}Z^{E}_{k9}+A^*_{Yye}Z^{E,*}_{j9}Z^{E}_{k10}\Big)Z^{H}_{i2}\\
&-2\sqrt{2}\Big(A_{e,ab}Z^{E}_{k4+a}Z^{E,*}_{jb}+A^*_{e,ab}Z^{E,*}_{j4+a}Z^{E}_{kb}\Big)Z^{H}_{i1}\\
&+2\sqrt{2}\Big(Z^{E,*}_{jb}\mu^*Y_{e,ab}Z^{E}_{k4+a}+Z^{E,*}_{j4+a}\mu Y^*_{e,ab}Z^{E}_{kb}\Big)Z^{H}_{i2}\\
&+2\sqrt{2}Y_{ye}\Big(\mu^*Z^{E,*}_{j10}Z^{E}_{k9}+\mu Z^{E,*}_{j9}Z^{E}_{k10}\Big)Z^{H}_{i1}\\
&+2\sqrt{2}\Big(M_{yl,a}Y_{e,ba}Z^{E,*}_{j9}Z^{E}_{k4+b}-M_{ye,a}Y^*_{e,ab}Z^{E,*}_{j10}Z^{E}_{kb}\Big)Z^{H}_{i1}\\
&+2\sqrt{2}\Big(M_{yl,a}Y^*_{e,ba}Z^{E,*}_{j4+b}Z^{E}_{k9}-M_{ye,a}Y_{e,ab}Z^{E,*}_{jb}Z^{E}_{k10}\Big)Z^{H}_{i1}\\
&+2\sqrt{2}Y_{ye}\Big(M_{yl,a}Z^{E,*}_{j10}Z^{E}_{ka}-M_{ye,a}Z^{E,*}_{j9}Z^{E}_{k4+a}\Big)Z^{H}_{i2}\\
&+2\sqrt{2}Y_{ye}\Big(Z^{E,*}_{ja}M_{yl,a}Z^{E}_{k10}-Z^{E,*}_{j4+a}M_{ye,a}Z^{E}_{k9}\Big)Z^{H}_{i2}\\
&-4v_uY^2_{ye}\Big(Z^{E,*}_{j9}Z^{E}_{k9}-Z^{E,*}_{j10}Z^{E}_{k10}\Big)Z^{H}_{i2}\\
&-4v_d\Big(Z^{E,*}_{j4+c}Y^*_{e,ca}Y_{e,ba}Z^{E}_{k4+b}+Z^{E,*}_{jb}Y^*_{e,ac}Y_{e,ab}Z^{E}_{kc}\Big)Z^{H}_{i1}\\
&+\Big[\Big(g_1^2-g_2^2\Big)Z^{E,*}_{j9}Z^{E}_{k9}-2g_1^2Z^{E,*}_{j10}Z^{E}_{k10}\Big]\Big(v_dZ^{H}_{i1}-v_uZ^{H}_{i2}\Big)\\
&+\Big[\Big(g_2^2-g_1^2\Big)\Big)Z^{E,*}_{ja}Z^{E}_{ka}+2g_1^2Z^{E,*}_{j4+a}Z^{E}_{k4+a}\Big]\Big(v_dZ^{H}_{i1}-v_uZ^{H}_{i2}\Big)\Big)\Big\}
\end{aligned}$$

4. Sfermion-Gauge Boson

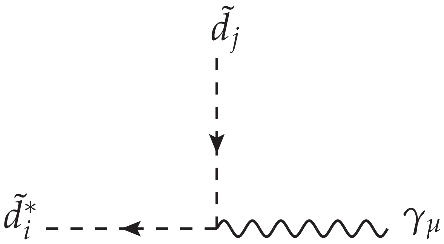

$$-i\frac{1}{3}e\Big(Z^{D,*}_{ia}Z^{D}_{ja}+Z^{D,*}_{i4+a}Z^{D}_{j4+a}-Z^{D,*}_{i9}Z^{D}_{j9}-Z^{D,*}_{i10}Z^{D}_{j10}\Big)\Big(p^{\tilde{d}^*_i}_\mu-p^{\tilde{d}_j}_\mu\Big)$$

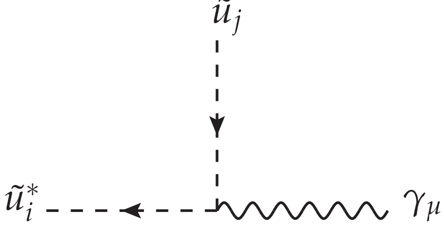

$$i\frac{2}{3}e\Big(Z^{U,*}_{ia}Z^{U}_{ja}+Z^{U,*}_{i4+a}Z^{U}_{j4+a}-Z^{U,*}_{i9}Z^{U}_{j9}-Z^{U,*}_{i10}Z^{U}_{j10}\Big)\Big(p^{\tilde{u}^*_i}_\mu-p^{\tilde{u}_j}_\mu\Big)$$

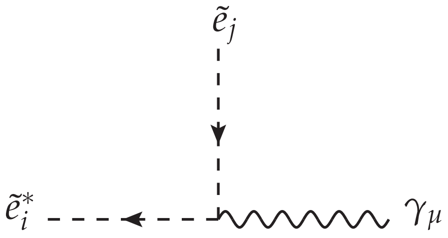

$$-ie\Big(Z^{E,*}_{ia}Z^{E}_{ja}+Z^{E,*}_{i4+a}Z^{E}_{j4+a}-Z^{E,*}_{i9}Z^{E}_{j9}-Z^{E,*}_{i10}Z^{E}_{j10}\Big)\Big(p^{\tilde{e}^*_i}_\mu-p^{\tilde{e}_j}_\mu\Big)$$

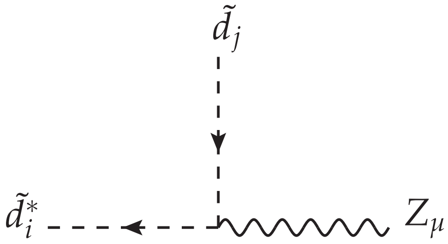

$$\frac{ie}{3\sin 2\Theta_W}\Big(\Big(3-2\sin^2\Theta_W\Big)Z^{D,*}_{ia}Z^{D}_{ja}-2\sin^2\Theta_W Z^{D,*}_{i4+a}Z^{D}_{j4+a}$$
$$-\Big(3-2\sin^2\Theta_W\Big)Z^{D,*}_{i9}Z^{D}_{j9}+2\sin^2\Theta_W Z^{D,*}_{i10}Z^{D}_{j10}\Big)\Big(p^{\tilde{d}^*_i}_\mu-p^{\tilde{d}_j}_\mu\Big)$$

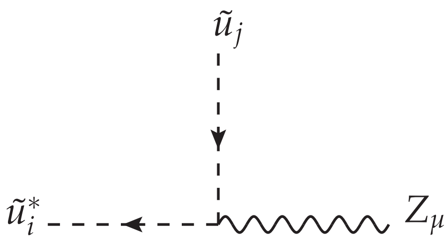

$$-\frac{ie}{3\sin^2\Theta_W}\Big(\Big(3-4\sin^2\Theta_W\Big)Z^{U,*}_{ia}Z^{U}_{ja}-4\sin^2\Theta_W Z^{U,*}_{i4+a}Z^{U}_{j4+a}$$
$$-\Big(3-4\sin^2\Theta_W\Big)Z^{U,*}_{i9}Z^{U}_{j9}+4\sin^2\Theta_W Z^{U,*}_{i10}Z^{U}_{j10}\Big)\Big(p^{\tilde{u}^*_i}_\mu-p^{\tilde{u}_j}_\mu\Big)$$

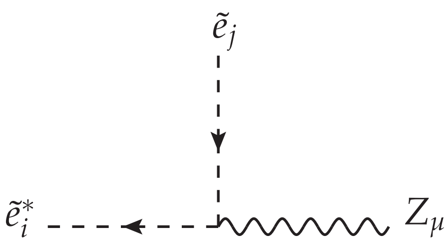

$$\frac{ie}{\sin 2\Theta_W}\Big(\Big(1-2\sin^2\Theta_W\Big)Z^{E,*}_{ia}Z^{E}_{ja}-2\sin^2\Theta_W Z^{E,*}_{i4+a}Z^{E}_{j4+a}$$
$$-\Big(1-2\sin^2\Theta_W\Big)Z^{E,*}_{i9}Z^{E}_{j9}+2\sin^2\Theta_W Z^{E,*}_{i10}Z^{E}_{j10}\Big)\Big(p^{\tilde{e}^*_i}_\mu-p^{\tilde{e}_j}_\mu\Big)$$

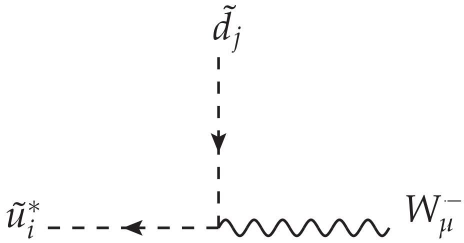

$$-i\frac{1}{\sqrt{2}}g_2\Big(Z^{U,*}_{ia}Z^{D}_{ja}+Z^{U,*}_{i9}Z^{D}_{j9}\Big)\Big(p^{\tilde{u}^*_i}_\mu-p^{\tilde{d}_j}_\mu\Big)$$

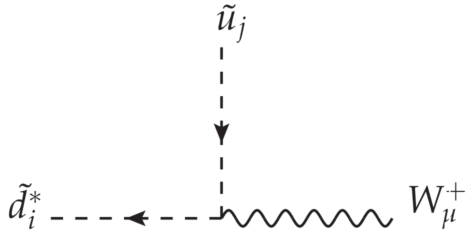

$$-i\frac{1}{\sqrt{2}} g_2 \Big(Z^{D,*}_{ia} Z^{U}_{ja} + Z^{D,*}_{i9} Z^{U}_{j9}\Big)\Big(p^{\tilde{d}_i^*}_\mu - p^{\tilde{u}_j}_\mu\Big)$$

5. Chargino/Neutralino-Fermion and Sfermion

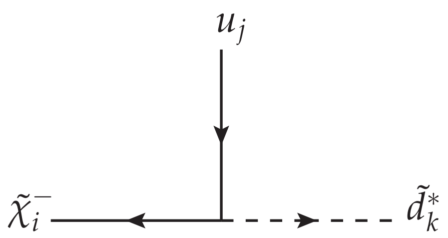

$$-i\Big(g_2 U^*_{i1} U^{u,*}_{L,ja} Z^D_{ka} - Y_{yu} U^*_{i2} U^{u,*}_{L,j5} Z^D_{k9} - \sum_{a=1}^{4} Y_{d,ab} U^*_{i2} U^{u,*}_{L,jb} Z^D_{k4+a}\Big) P_L$$
$$-i\Big(g_2 V_{i1} U^u_{R,j5} Z^D_{k9} - Y_{yd} V_{i2} U^u_{R,j5} Z^D_{k10} - sum^4_{b=1} Y^*_{u,ab} V_{i2} U^u_{R,ja} Z^D_{kb}\Big) P_R$$

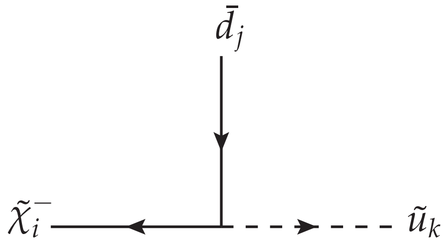

$$-i\Big(g_2 U^{d,*}_{R,j5} Z^{U,*}_{k9} U^*_{i1} - Y_{yu} U^{d,*}_{R,j5} Z^{U,*}_{k10} U^*_{i2} - \sum_{b=1}^{4} Y_{d,ab} U^{d,*}_{R,ja} Z^{U,*}_{kb} U^*_{i2}\Big) P_L$$
$$-i\Big(g_2 U^d_{L,ja} Z^{U,*}_{ka} V_{i1} - Y_{yd} U^d_{L,j5} Z^{U,*}_{k9} V_{i2} - \sum_{a=1}^{4} Y^*_{u,ab} U^d_{L,jb} Z^{U,*}_{k4+a} V_{i2}\Big) P_R$$

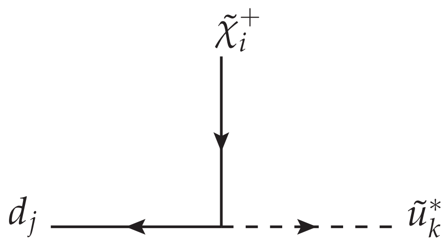

$$-i\Big(g_2 Z^U_{ka} U^{d,*}_{L,ja} V^*_{i1} - Y_{yd} Z^U_{k9} U^{d,*}_{L,j5} V^*_{i2} - Z^U_{k4+a} U^{d,*}_{L,jb} Y_{u,ab} V^*_{i2}\Big) P_L$$
$$-i\Big(g_2 Z^U_{k9} U^d_{R,j5} U_{i1} - Y_{yu} Z^U_{k10} U^d_{R,j5} U_{i2} - Z^U_{kb} U^d_{R,ja} Y^*_{d,ab} U_{i2}\Big) P_R$$

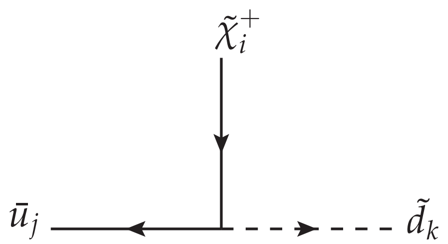

$$-i\Big(g_2 Z^{D,*}_{k9} U^{u,*}_{R,j5} V^*_{i1} - Y_{yd} Z^{D,*}_{k10} U^{u,*}_{R,j5} V^*_{i2} - Z^{D,*}_{kb} U^{u,*}_{R,ja} Y_{u,ab} V^*_{i2}\Big) P_L$$
$$-i\Big(g_2 Z^{D,*}_{ka} U^u_{L,ja} U_{i1} - Y_{yu} Z^{D,*}_{k9} U^u_{L,j5} U_{i2} - Z^{D,*}_{k4+a} U^u_{L,jb} Y^*_{d,ab} U_{i2}\Big) P_R$$

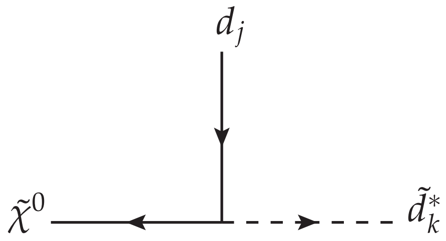

$$\frac{i}{6}\Big(3\sqrt{2}g_2 N^*_{i2} U^{d,*}_{L,ja} Z^D_{ka} - 6 N^*_{i3} U^{d,*}_{L,jb} Y_{d,ab} Z^D_{k4+a}$$
$$-6 Y_{yd} U^{d,*}_{L,j5} N^*_{i4} Z^D_{k9} + 2\sqrt{2} g_1 N^*_{i1} U^{d,*}_{L,j5} Z^D_{k10} - \sqrt{2} g_1 N^*_{i1} U^{d,*}_{L,ja} Z^D_{ka}\Big) P_L$$
$$-\frac{i}{6}\Big(3\sqrt{2} g_2 Z^D_{k9} U^d_{R,j5} N_{i2} + 6 Y^*_{d,ab} U^d_{R,ja} Z^D_{kb} N_{i3}$$
$$+6 Y_{yd} Z^D_{k10} U^d_{R,j5} N_{i4} + 2\sqrt{2} g_1 \sum_{a=1}^{4} Z^D_{k4+a} U^d_{R,ja} N_{i1} - \sqrt{2} g_1 Z^D_{k9} U^d_{R,j5} N_{i1}\Big) P_R$$

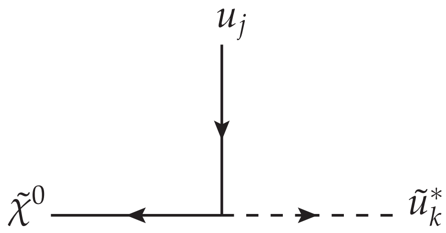

$$-\frac{i}{6}\Big(3\sqrt{2} g_2 N^*_{i2} U^{u,*}_{L,ja} Z^U_{ka} + 6 N^*_{i4} U^{u,*}_{L,jb} Y_{u,ab} Z^U_{k4+a}$$
$$+6 Y_{yu} N^*_{i3} U^{u,*}_{L,j5} Z^U_{k9} + 4\sqrt{2} g_1 N^*_{i1} U^{u,*}_{L,j5} Z^U_{k10} + \sqrt{2} g_1 N^*_{i1} U^{u,*}_{L,ja} Z^U_{ka}\Big) P_L$$
$$+\frac{i}{6}\Big(3\sqrt{2} g_2 N_{i2} Z^U_{k9} U^u_{R,j5} - 6 Y^*_{u,ab} U^u_{R,ja} Z^U_{kb} N_{i4}$$
$$-6 Y_{yu} N_{i3} Z^U_{k10} U^u_{R,j5} + 4\sqrt{2} g_1 Z^U_{k4+a} U^u_{R,ja} N_{i1} + \sqrt{2} g_1 N_{i1} Z^U_{k9} U^u_{R,j5}\Big) P_R$$

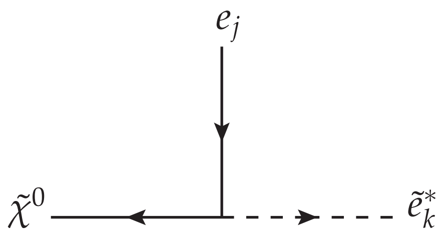

$$\frac{i}{2}\Big(\sqrt{2} g_2 N^*_{i2} U^{e,*}_{L,ja} Z^E_{ka} - 2 N^*_{i3} U^{e,*}_{L,jb} Y_{e,ab} Z^E_{k4+a}$$
$$-2 Y_{ye} N^*_{i4} U^{e,*}_{L,j5} Z^E_{k9} + 2\sqrt{2} g_1 N^*_{i1} U^{e,*}_{L,j5} Z^E_{k10} + \sqrt{2} g_1 N^*_{i1} U^{e,*}_{L,ja} Z^E_{ka}\Big) P_L$$
$$-\frac{i}{2}\Big(\sqrt{2} g_2 Z^E_{k9} U^e_{R,j5} N_{i2} + 2 Y^*_{e,ab} U^e_{R,ja} Z^E_{kb} N_{i3}$$
$$+2 Y^*_{ye} Z^E_{k10} U^e_{R,j5} N_{i4} + \sqrt{2} g_1 Z^E_{k9} U^e_{R,j5} N_{i1} + 2\sqrt{2} g_1 Z^E_{k4+a} U^e_{R,ja} N_{i1}\Big) P_R$$

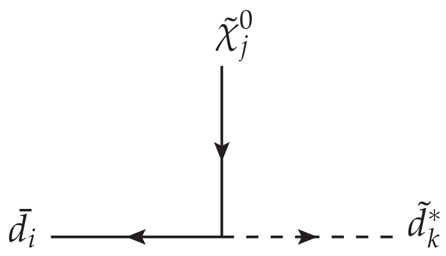

$$-\frac{i}{6}\Big(6 Z^{D,*}_{kb} Y_{d,ab} U^{d,*}_{R,ia} N^*_{j3} + 6 Y_{yd} Z^{D,*}_{k10} U^{d,*}_{R,i5} N^*_{j4}$$
$$+3\sqrt{2} g_2 Z^{D,*}_{k9} U^{d,*}_{R,i5} N^*_{j2} - \sqrt{2} g_1 Z^{D,*}_{k9} U^{d,*}_{R,i5} N^*_{j1} + 2\sqrt{2} g_1 Z^{D,*}_{k4+a} U^{d,*}_{R,ia} N^*_{j1}\Big) P_L$$
$$-\frac{i}{6}\Big(6 Z^{D,*}_{k4+a} Y^*_{d,ab} U^d_{L,ib} N_{j3} + 6 Y_{yd} Z^{D,*}_{k9} U^d_{L,i5} N_{j4}$$
$$-3\sqrt{2} g_2 Z^{D,*}_{ka} U^d_{L,ia} N_{j2} + \sqrt{2} g_1 Z^{D,*}_{ka} U^d_{L,ia} N_{j1} - 2\sqrt{2} g_1 Z^{D,*}_{k10} U^d_{L,i5} N_{j1}\Big) P_R$$

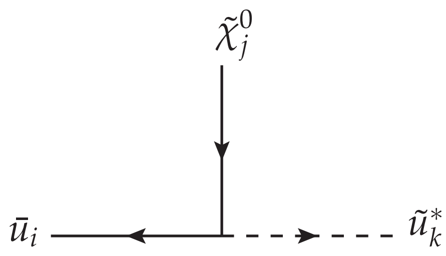

$$-\frac{i}{6}\Big(6 U^{u,*}_{R,ia} Y_{u,ab} Z^{U,*}_{kb} N^*_{j4} - 4\sqrt{2} g_1 Z^{U,*}_{k4+a} U^{u,*}_{R,ia} N^*_{j1}$$
$$-\sqrt{2} g_1 Z^{U,*}_{k9} U^{u,*}_{R,i5} N^*_{j1} - 3\sqrt{2} g_2 Z^{U,*}_{k9} U^{u,*}_{R,i5} N^*_{j2} + 6 Y_{yu} Z^{U,*}_{k10} U^{u,*}_{R,i5} N^*_{j3}\Big) P_L$$
$$-\frac{i}{6}\Big(6 Z^{U,*}_{k4+a} Y^*_{u,ab} U^u_{L,ib} N_{j4} + 4\sqrt{2} g_1 Z^{U,*}_{k10} U^u_{L,i5} N_{j1}$$
$$+\sqrt{2} g_1 Z^{U,*}_{ka} U^u_{L,ia} N_{j1} + 3\sqrt{2} g_2 Z^{U,*}_{ka} U^u_{L,ia} N_{j2} + 6 Y_{yu} Z^{U,*}_{k9} U^u_{L,i5} N_{j3}\Big) P_R$$

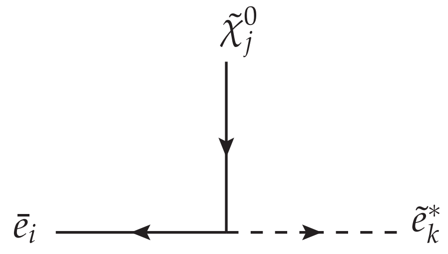

$$
\begin{aligned}
&-\frac{i}{2}\Big(2\sqrt{2}g_1 Z^{E,*}_{k4+a} U^{e,*}_{R,ia} N^*_{j1} + 2\sum_{a=1}^{4} Z^{E,*}_{kb} U^{e,*}_{R,ia} Y_{e,ab} N^*_{j3} \\
&+\sqrt{2}g_1 Z^{E,*}_{k9} U^{e,*}_{R,i5} N^*_{j1} + \sqrt{2}g_2 Z^{E,*}_{k9} U^{e,*}_{R,i5} N^*_{j2} + 2Y_{ye} Z^{E,*}_{k10} U^{e,*}_{R,i5} N^*_{j4}\Big) P_L \\
&+\frac{i}{2}\Big(2\sqrt{2}g_1 Z^{E,*}_{k10} U^{e}_{L,i5} N_{j1} - 2Z^{E,*}_{k4+a} U^{e}_{L,ib} Y^*_{e,ab} N_{j3} \\
&+\sqrt{2}g_1 Z^{E,*}_{ka} U^{e}_{L,ia} N_{j1} + \sqrt{2}g_2 Z^{E,*}_{ka} U^{e}_{L,ia} N_{j2} - 2Y^*_{ye} Z^{E,*}_{k9} U^{e}_{L,i5} N_{j4}\Big) P_R
\end{aligned}
$$

References

[1] G. Aad *et al.* [ATLAS Collaboration], Phys. Lett. B **716**, 1 (2012) [arXiv:1207.7214 [hep-ex]].

[2] S. Chatrchyan *et al.* [CMS Collaboration], Phys. Lett. B **716**, 30 (2012) [arXiv:1207.7235 [hep-ex]].

[3] S. M. Barr, Phys. Lett. B **112**, 219 (1982).

[4] J. P. Derendinger, J. E. Kim and D. V. Nanopoulos, Phys. Lett. B **139**, 170 (1984).

[5] I. Antoniadis, J. R. Ellis, J. S. Hagelin and D. V. Nanopoulos, Phys. Lett. B **194**, 231 (1987).

[6] J. Jiang, T. Li, D. V. Nanopoulos and D. Xie, Phys. Lett. B **677**, 322 (2009); Nucl. Phys. B **830**, 195 (2010).

[7] J. Jiang, T. Li and D. V. Nanopoulos, Nucl. Phys. B **772**, 49 (2007).

[8] I. Antoniadis, J. R. Ellis, J. S. Hagelin and D. V. Nanopoulos, Phys. Lett. B **208**, 209 (1988) [Addendum-ibid. B **213**, 562 (1988)]; Phys. Lett. B **231**, 65 (1989).

[9] J. L. Lopez, D. V. Nanopoulos and K. J. Yuan, Nucl. Phys. B **399**, 654 (1993).

[10] C. Beasley, J. J. Heckman and C. Vafa, JHEP **0901**, 058 (2009); JHEP **0901**, 059 (2009); R. Donagi and M. Wijnholt, arXiv:0802.2969 [hep-th]; arXiv:0808.2223 [hep-th].

[11] K. Nakamura, Int. J. Mod. Phys. A **18**, 4053 (2003).

[12] S. Raby *et al.*, arXiv:0810.4551 [hep-ph].

[13] T. Li, D. V. Nanopoulos and J. W. Walker, Phys. Lett. B **693**, 580 (2010).

[14] T. Li, D. V. Nanopoulos and J. W. Walker, Nucl. Phys. B **846**, 43 (2011) [arXiv:1003.2570 [hep-ph]].

[15] B. Kyae and Q. Shafi, Phys. Lett. B **635**, 247 (2006) [arXiv:hep-ph/0510105].

[16] Y. Huo, T. Li, D. V. Nanopoulos and C. Tong, arXiv:1109.2329 [hep-ph].

[17] T. Li, J. A. Maxin, D. V. Nanopoulos and J. W. Walker, Phys. Lett. B **710**, 207 (2012) [arXiv:1112.3024 [hep-ph]].

[18] E. Cremmer, S. Ferrara, C. Kounnas and D. V. Nanopoulos, Phys. Lett. B **133**, 61 (1983); J. R. Ellis, A. B. Lahanas, D. V. Nanopoulos and K. Tamvakis, Phys. Lett. B **134**, 429 (1984); J. R. Ellis, C. Kounnas and D. V. Nanopoulos, Nucl. Phys. B **241**, 406 (1984); Nucl. Phys. B **247**, 373 (1984); A. B. Lahanas and D. V. Nanopoulos, Phys. Rept. **145**, 1 (1987).

[19] T. Li, J. A. Maxin, D. V. Nanopoulos and J. W. Walker, Phys. Rev. D **83**, 056015 (2011) [arXiv:1007.5100 [hep-ph]].

[20] T. Li, J. A. Maxin, D. V. Nanopoulos and J. W. Walker, Phys. Lett. B **699**, 164 (2011) [arXiv:1009.2981 [hep-ph]].

[21] T. Li, J. A. Maxin, D. V. Nanopoulos and J. W. Walker, arXiv:1202.0509 [hep-ph].

[22] T. Li, D. V. Nanopoulos, W. -Y. Wang, X. -C. Wang and Z. -H. Xiong, JHEP **1207**, 190 (2012) [arXiv:1204.5326 [hep-ph]].

[23] S. P. Martin, Phys. Rev. D **75**, 055005 (2007) [hep-ph/0701051].

[24] K. S. Babu, I. Gogoladze, M. U. Rehman and Q. Shafi, Phys. Rev. D **78**, 055017 (2008) [arXiv:0807.3055 [hep-ph]].

[25] S. P. Martin, Phys. Rev. D **81**, 035004 (2010) [arXiv:0910.2732 [hep-ph]].

[26] P. W. Graham, A. Ismail, S. Rajendran and P. Saraswat, Phys. Rev. D **81**, 055016 (2010) [arXiv:0910.3020 [hep-ph]].

[27] X. Chang and R. Huo, Phys. Rev. D **89**, 036005 (2014) [arXiv:1402.4204 [hep-ph]].

[28] K. Nickel and F. Staub, arXiv:1505.06077 [hep-ph].

[29] F. Staub, Comput. Phys. Commun. **185**, 1773 (2014) [arXiv:1309.7223 [hep-ph]].

[30] A. Dabelstein, Z. Phys. C **67**, 495 (1995) [hep-ph/9409375].